

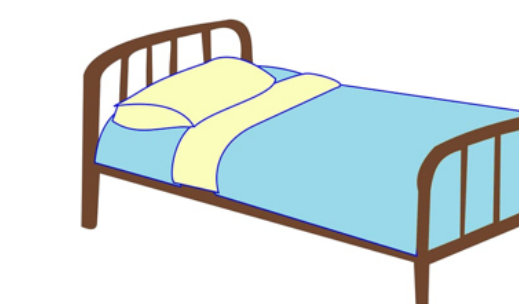
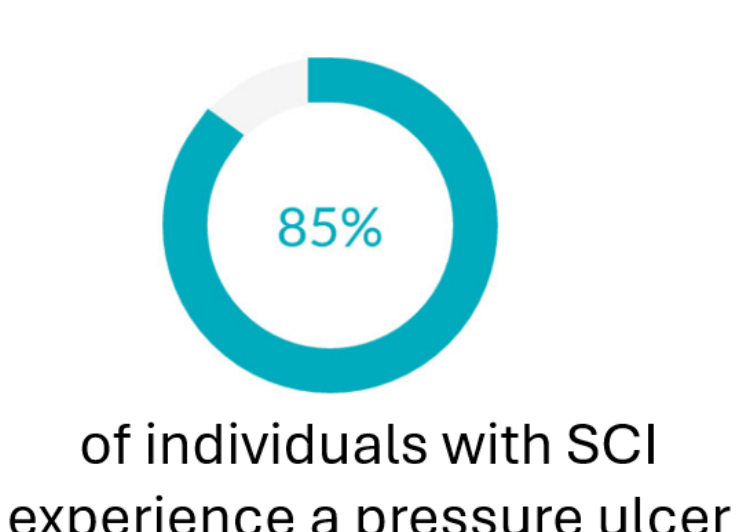
PressurePro: Wheelchair Cushion Inflation Control System

Team 17: Sophie Stupalo, Eve Boulanger, Inaara Ahmed-Fazal, Meghan LaCoste, and Hannah Cardoza

Background & Motivation

Pressure Ulcers Among Wheelchair Users:

Pressure ulcers that develop underneath the sit bones (ischial region) are the most common health complication among wheelchair users [1]. They are especially common among those with complete spinal cord injuries due to their lack of sensation and mobility.



Recovery can take up to several months at home, in a long-term care facility, or in hospital [3]

The cost of healing a pressure ulcer can range from \$500 to \$70000 [4]

Stakeholders: Individuals with complete spinal cord injuries, other wheelchair users, caregivers, occupational therapists

Limitations of Current Solutions :

The ROHO® Quadro Select® is one of the most commonly prescribed wheelchair cushions for individuals who are at a higher risk of developing an ulcer [5]. It sets itself apart by its ability to distribute pressure independently amongst its four quadrants.



However, it is only effective at certain inflation level specific to each patient, as determined by an occupational therapist. This level of inflation is difficult to maintain due to the prevalence of leaks [5]. Both over and underinflation of the cushion increases the risk of pressure ulcers [6].

Currently, users are required to manually and subjectively check and correct inflation levels, requiring physical effort, mobility and daily adherence [6]. This also leaves them vulnerable to leaks that occur in less than one day, as unsafe inflation levels can lead to pressure ulcers within hours [6].

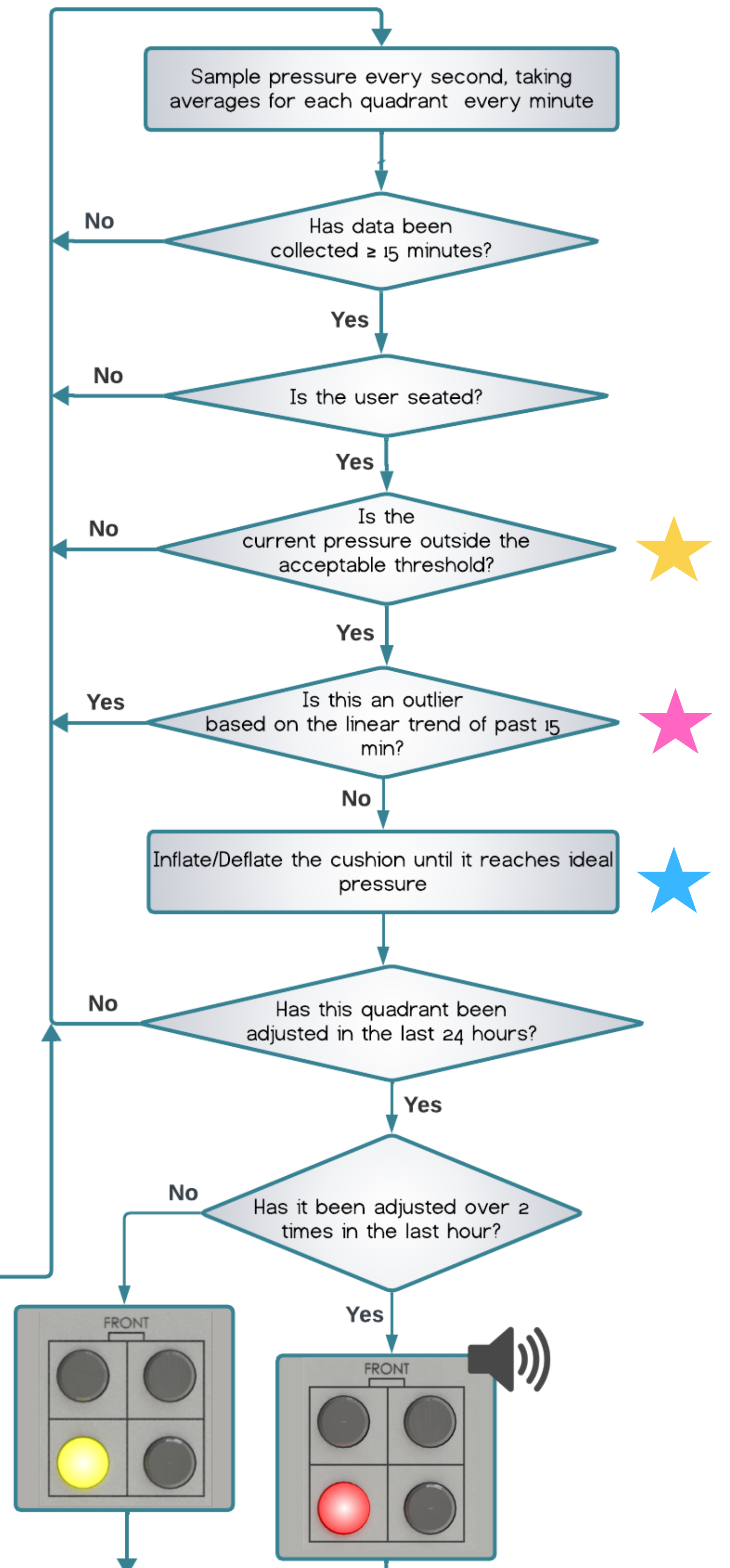
The most common cause of adverse events and pressure ulcers for the ROHO® Quadro Select® is the failure to maintain safe inflation levels [7].

Project Objectives

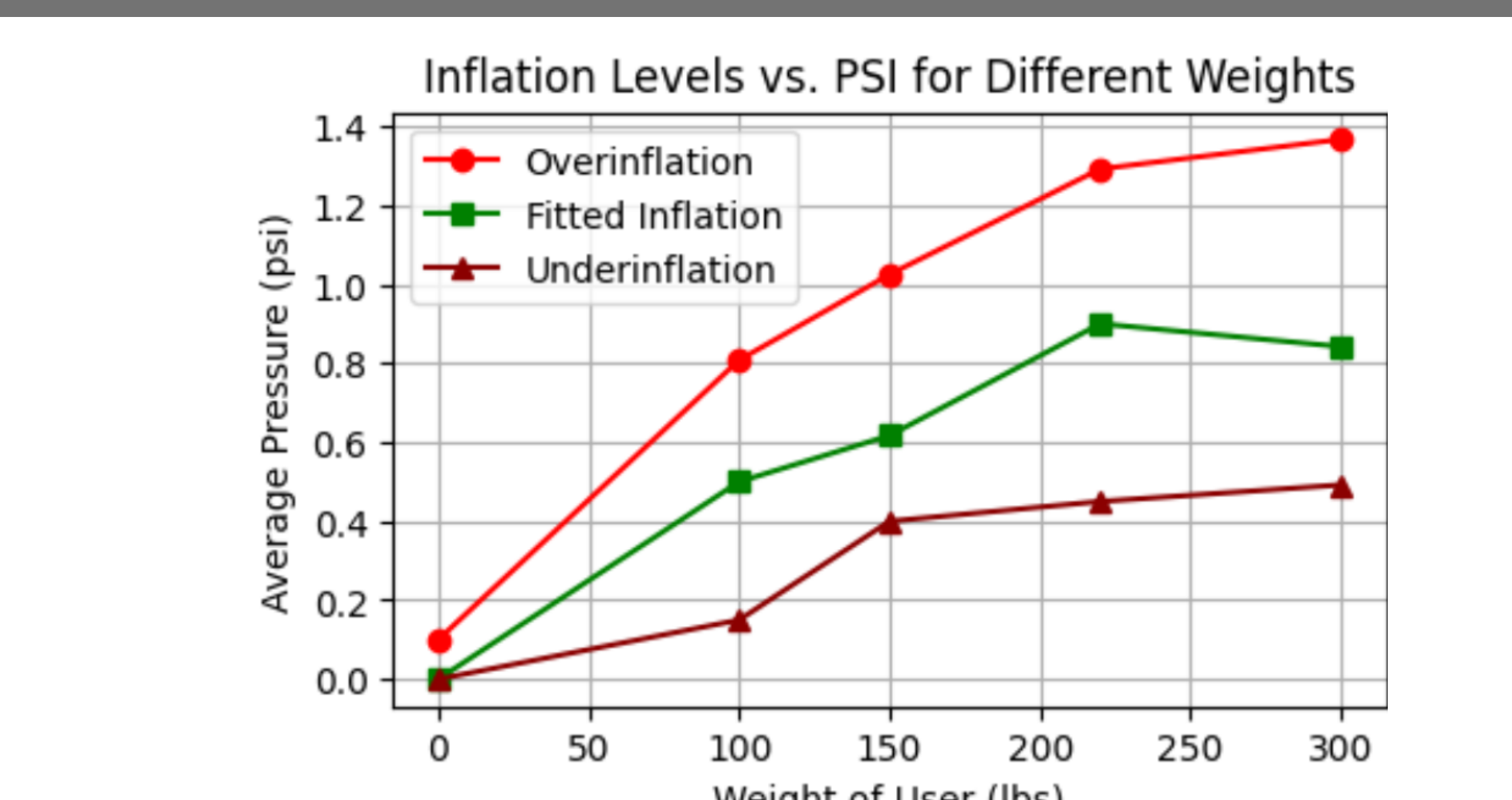
Design attachment for ROHO® Quadro Select® Cushion that reduces risk of pressure ulcers by:

1. Continuously monitoring and correcting internal pressure levels to OT recommendation
2. Alerting users of quadrants with leaks for repair

Logic Flowchart



Mapping Pressure to Inflation



Designed Solution



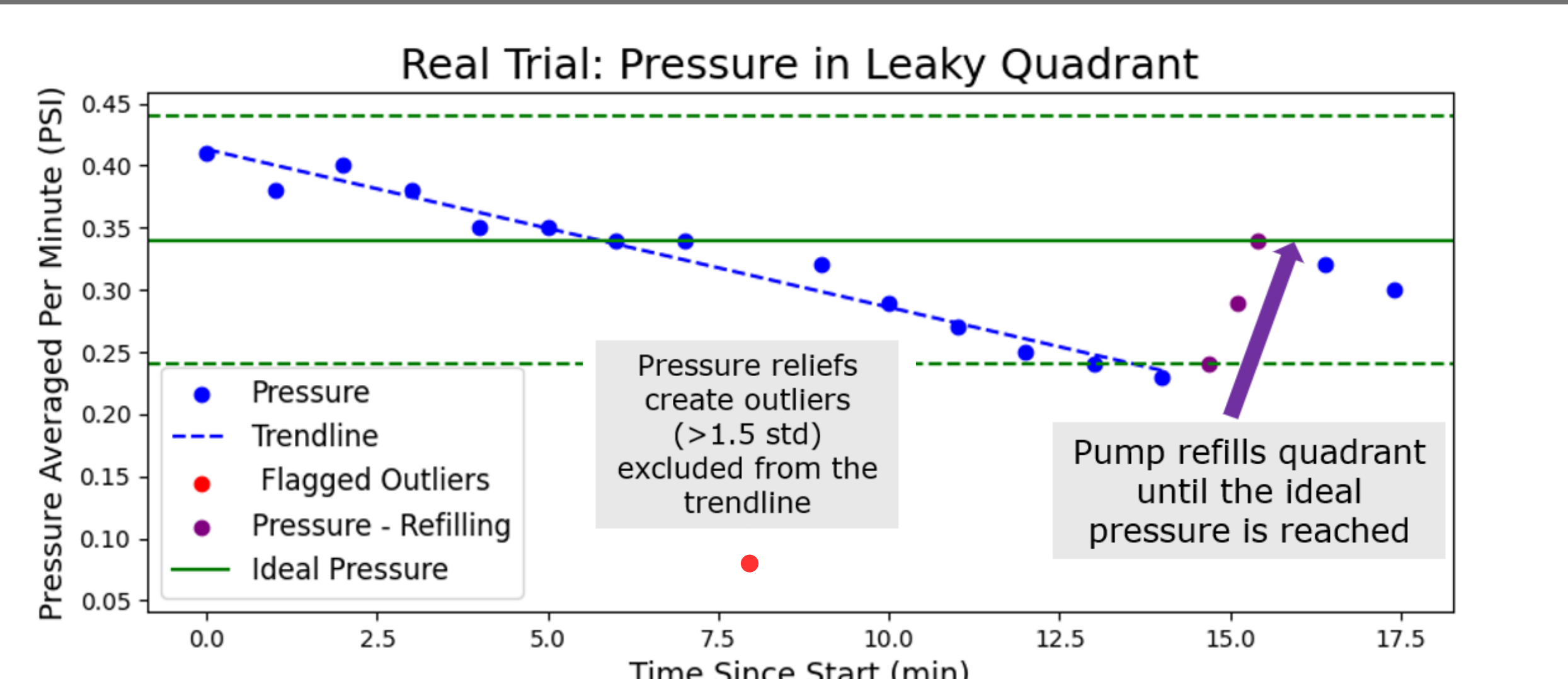
Determining Outliers

The algorithm had to differentiate real leaks from pressure reliefs and system noise when determining when to adjust inflation.

We determined that a linear trend of the past 15 minutes had the best specificity and quickest response time on sets of simulated data ranging in noise and leak rates. Pressure readings that do not align with the trend of the past 15 minutes are classified as outliers.

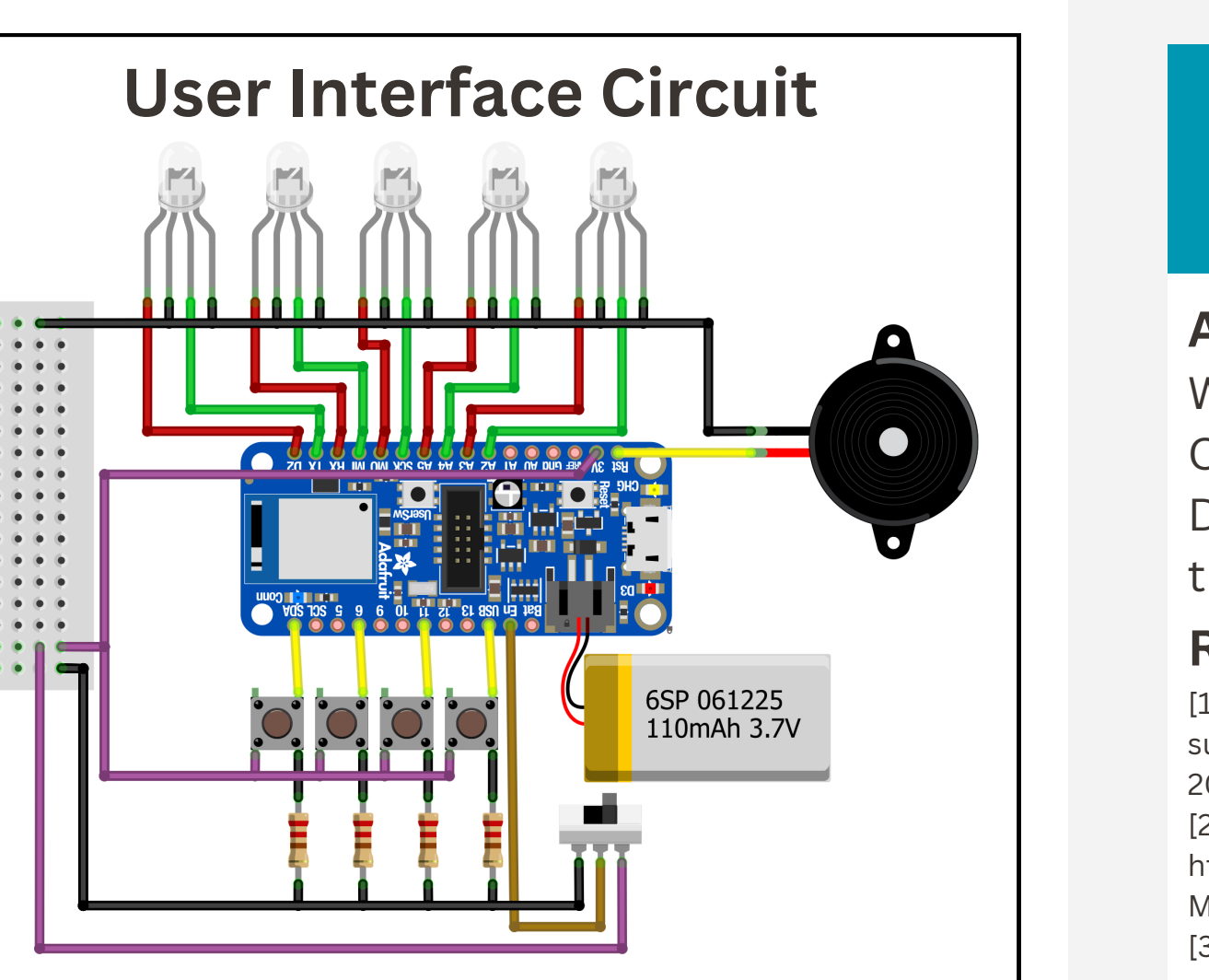
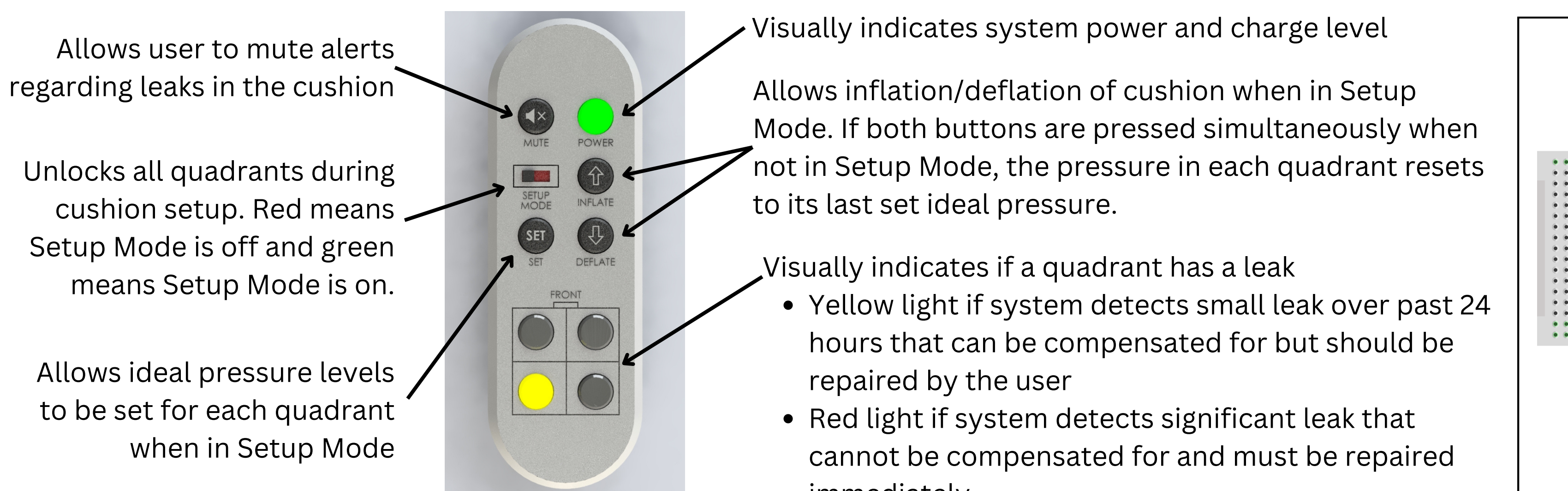


Correcting Dangerous Pressure levels

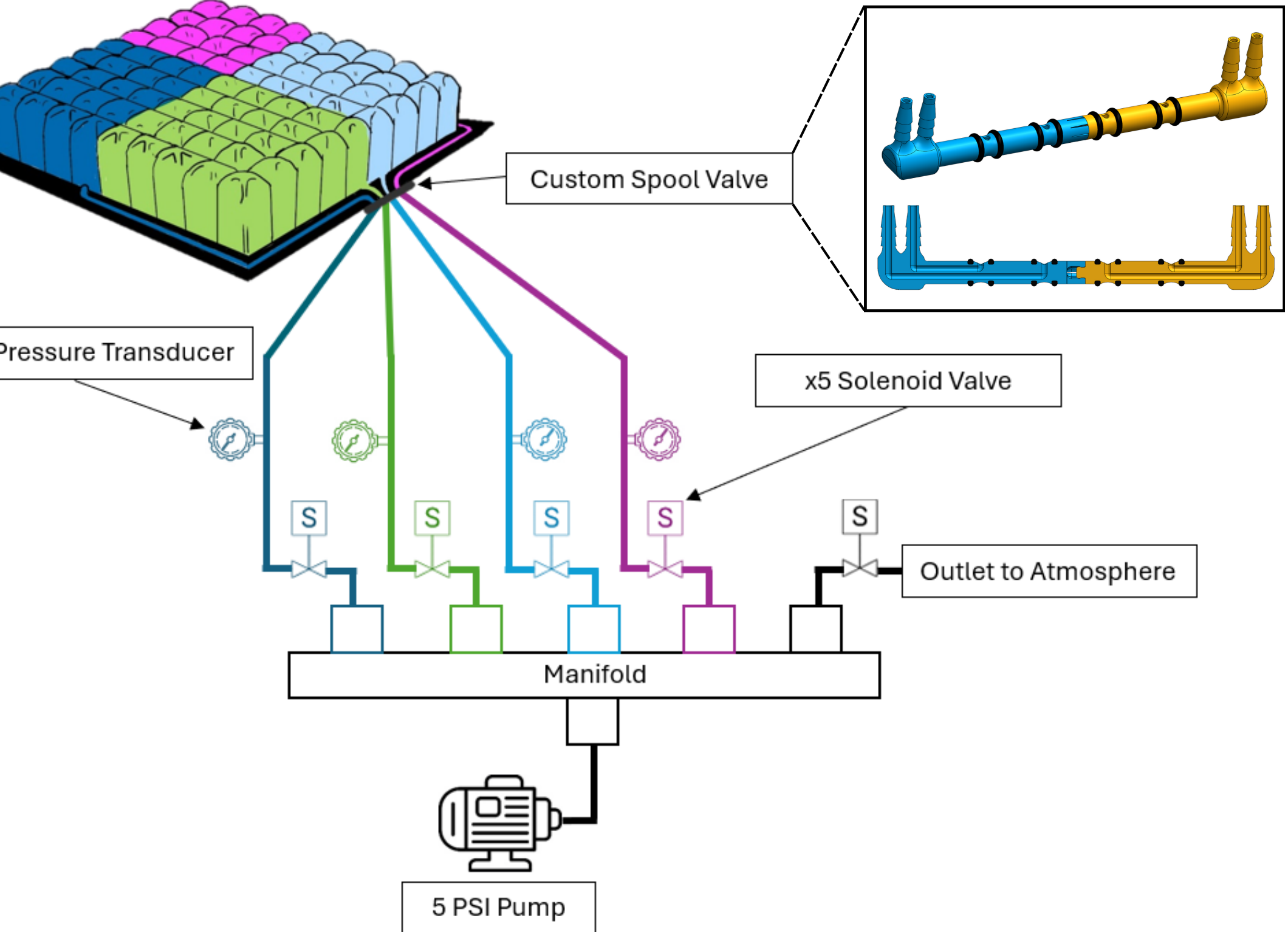


The system approximates the pump time required to fix the difference in pressure. After each interval it pauses to sense the error, repeating until the error is less than 0.01 PSI.

User Interface



Mechanical/Pneumatic System

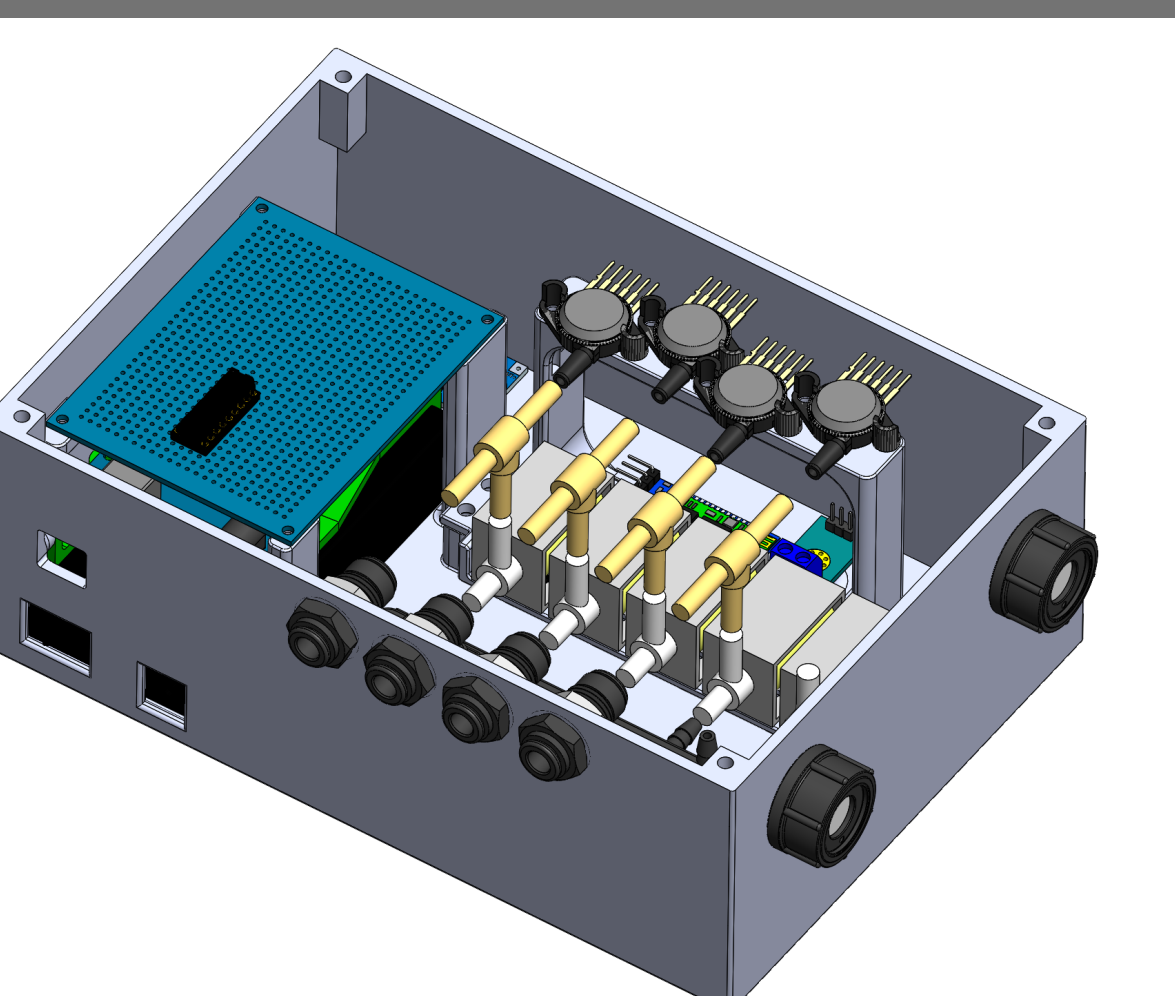


The solution is a low-pressure (<3 psi) pneumatic system which detects the pressure in each quadrant of the cushion and can inflate or deflate as needed.

Starting from the cushion, a custom spool valve is used to access each quadrant separately. The pressure in each quadrant is then measured using pressure transducers. Based on these readings, an algorithm controls the opening and closing of solenoid valves which control the channels to specific quadrants. The algorithm also switches the air pump on and off.

If deflation is required, the outlet valve and the valve connected to the specified quadrant are opened to expel excess air to the atmosphere.

Device Housing



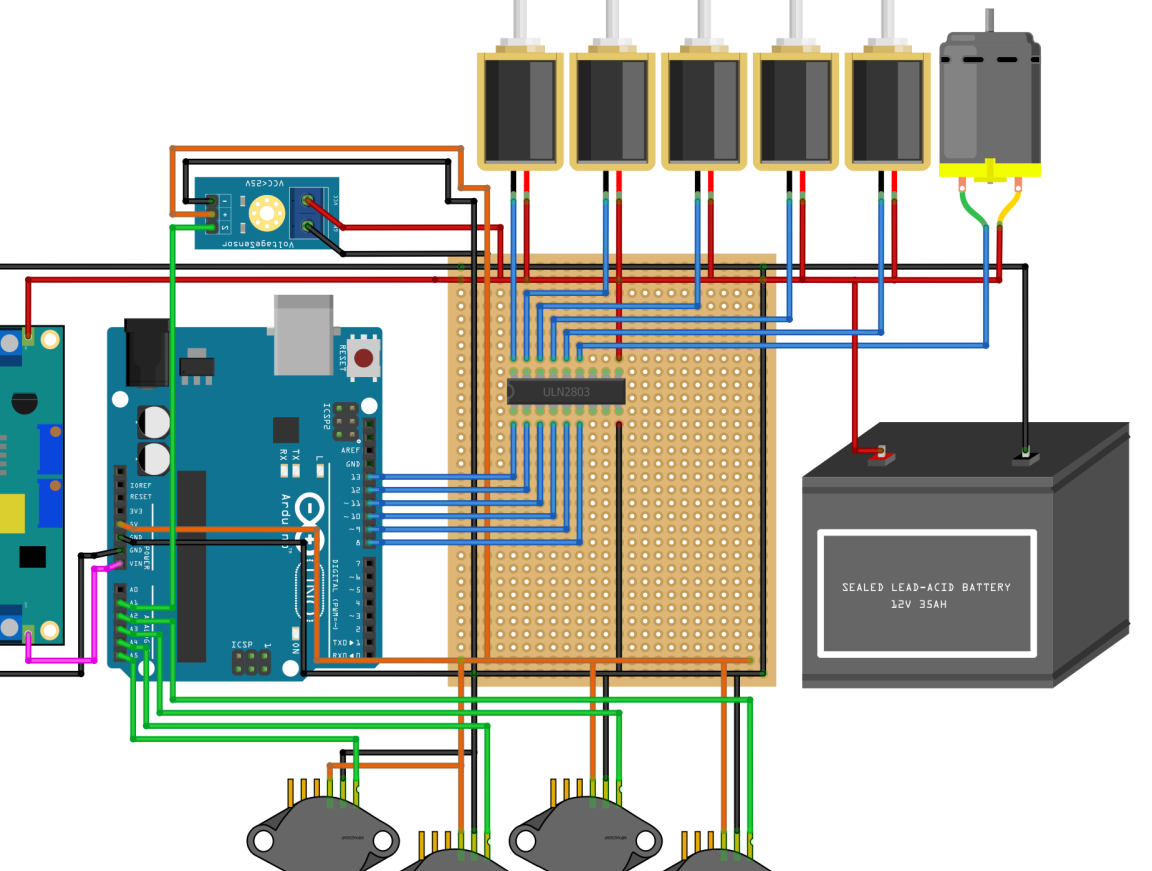
The mechanical/electrical system is housed compactly underneath the seat of the wheelchair through straps. One can quickly and easily separate these parts from the cushion if needed for leak repair.

This system communicates to the user interface, which can be attached to the armrest, for easy access to controls and visual indications.

Electrical System

The electrical system connects the sensors, solenoid valves, and pump to a Darlington transistor, Arduino, and a battery to be able to power and control the components.

The pump and solenoid valves are controlled using a Darlington transistor. The pressure transducers are connected to an Arduino Uno which receives pressure data from the cushion. The whole system is powered by a 12V battery which is stepped down to 9V via a voltage regulator to power the Arduino. The 5V source from the Arduino Uno is used to power the smaller components.



References & Affiliations

Acknowledgements:

We thank Professor Jenny Howcroft for her invaluable support as our advisor and for facilitating our engagement with stakeholders via the Stakeholder Café. Our gratitude also extends to permobil for their generous cushion donation as well as funding we received through the Baylis Medical Capstone Design Award and the Canadian Posture & Seating Centre Scholarship. Special thanks to Alex Magdanz, Chris McClellan, Calvin Young, and Bryan Tripp for their expert guidance and mentorship throughout this project.

References:

- [1] Kasai, T., Isayama, and M. Sekido, "Squamous cell carcinoma arising from an ischial pressure ulcer initially suspected to be necrotizing soft tissue infection: A case report," Journal of Tissue Viability, vol. 30, no. 4, pp. 621-626, 2021.
- [2] "Pressure injury and Spinal Cord Injury," Pressure Injury Toolkit for Spinal Cord Injury and Spina Biifa, https://aci.health.nsw.gov.au/networks/spinal-cord-injury/pi-toolkit/pressure-injury-in-spinal-cord-injury accessed Mar. 18, 2024.
- [3] D. Fogelberg, M. Atkins, E. Blanche, M. Carlson, and F. Clark, "Decisions and dilemmas in everyday life: Daily use of wheelchairs by individuals with spinal cord injury and the impact on pressure ulcer risk," Topics in spinal cord rehabilitation, vol. 15, no. 2, pp. 16-32, 2009.
- [4] T. Boyko, M. T. Longaker, and G. P. Yang, "Review of the current management of pressure ulcers," Advances in Wound Care, vol. 7, no. 2, pp. 57-67, Feb. 2018. doi:10.1089/wound.2016.0697
- [5] S. Pritchard, H. Cardoza, and S. Stupalo, "Biomedical Stakeholder Café," In-Person Meeting (October 4, 2023).
- [6] J. Howcroft, E. Boulanger, and I. Ahmed-Fazal, "Biomedical Stakeholder Café," In-Person Meeting (October 3, 2023).
- [7] FDA, "Maude adverse event report: ROHO, Inc., ROHO® quadro select® high profile® cushion; wheelchair cushion," U.S. Food & Drug Administration, https://www.accessdata.fda.gov/scripts/cder/fdacmsatf/maude/device/detail.cfm?mfr_id=17720290&product_id=10420181&device_id=10420181&event_id=10420181 (accessed Nov. 9, 2023).

PressurePro: Automated Maintenance of Air Cushion Inflation for Pressure Ulcer Prevention

*Team 17: Eve Boulanger, Hannah Cardoza, Inaara Ahmed-Fazal,
Meghan LaCoste, Sophie Stupalo*

ABSTRACT

The PressurePro project is an automated system engineered to adjust and monitor the air pressure in an air-filled wheelchair cushion for individuals with complete spinal cord injuries, targeting the prevention of pressure ulcers. The device aims to address the limitations of the ROHO® High Profile Quadtro-Select cushion, by maintaining optimal inflation levels and notifying users of leaks to facilitate prompt repairs. Integrating pneumatic, mechanical, and electrical designs with an intuitive user interface, the PressurePro system shows promise in enhancing health outcomes, diminishing healthcare expenses, and boosting user autonomy. Recommendations for future development include enhancing battery efficiency, adapting components for traditional manufacturing methods, and refining the user interface for improved usability and compactness.

Keywords: Complete spinal cord injuries, pressure ulcers, ROHO® Cushion

1. INTRODUCTION

Pressure ulcers are localised injuries that result from prolonged pressure and shear forces that reduce capillary blood flow to tissues and cause tissue damage [1]. This can result in severe health consequences such as sepsis, tissue necrosis, as well as bone and joint infections [2]. Those with complete spinal cord injuries (SCI) are prone to developing pressure ulcers from lack of mobility, lack of sensation, prevalence of muscle atrophy, and incontinence [3]. The ischial region is the most common ulcer location [4]. Recovery can take weeks to months, often requiring the patient to be bedridden in long-term care facilities [5]. Treatment can put an economic strain on the healthcare system and patients with an average total treatment cost of \$118,700 per ulcer [6]. Wheelchair cushions that offer different pressure distributions are prescribed to individuals depending on their level of risk [7, 8]. The ROHO® High Profile Quadtro-Select® cushion (“the ROHO®”) by Permobil is one of the most commonly prescribed options for those at high risk of developing an ulcer [7]. It has proven to be more effective at reducing peak pressures than other competitors when used correctly [9, 10]. The ROHO® has flexible air cells that evenly distribute the user’s weight within the cushion’s four quadrants. To effectively mitigate pressure ulcer risks, the cushion must maintain a set level of inflation in each quadrant specific to the patient’s weight and postural asymmetry [7]. Occupational therapists (OT) determine the correct inflation level for the user and fit the cushion accordingly [7].

2. PROJECT MOTIVATION, SCOPE, AND OBJECTIVES

The main limitation of the ROHO® is that it is prone to tears and becomes porous over time [11]. These leaks are often small and thus difficult to notice, locate, and repair [7, 11]. Pressure ulcers resulting from improper inflation are the most common cause of adverse events reported by the FDA for the ROHO® [12, 13]. Users are instructed to perform a daily qualitative inflation level check by placing their hand under areas of high-pressure concentration and manually inflating or deflating the cushion as needed [7]. This process leaves room for user error, is highly dependent on daily adherence, and is not possible for the entire user population to perform due to lack of mobility. Even if these checks are performed

perfectly, users are still vulnerable to unexpected leaks that may cause them to reach unsafe inflation levels within a day. The motivation and scope for this project stem from these limitations; the final solution aims to address the aforementioned challenges to further prevent the risk of pressure ulcers.

The proposed solution has two main objectives: to continuously monitor and correct internal pressure levels to OT recommendations, and to alert users of any quadrant(s) with leaks to promote repair. The following situation impact statement was thus determined to be: “*Design a system for manual wheelchair users with complete spinal cord injuries who are prescribed air-filled cushions that reduces the risk of pressure ulcers by maintaining internal pressure levels of the ROHO® High Profile Quadtro-Select® cushion, as recommended by an occupational therapist.*”

3. SUMMARY OF ENGINEERING ANALYSIS & DESIGN METHODS

3.1 ENGINEERING SPECIFICATIONS

The non-functional requirements and their associated target values can be seen in Table A1 below. Justifications for the target values of R1, R2, R3, R5, R8, and R9 can be found in the final report from BME 461 [14]. R4 was modified to consider how long it takes to both attach and detach the ROHO® and PressurePro accessory from the wheelchair. Wheelchair accessories like the Quokka Mobility Bag, Handy Bag Under Bag, and SAMDEW Wheelchair Backpack can typically be installed within 1-2 minutes [15, 16, 17]. Thus, the target values for both the attachment (R4.1) and detachment (R4.2) time were set to 60 seconds. R6 was also modified based on the DALY and QALY estimates from the Economic Analysis report to have a target value of less than a 48.2% price increase [18]. R7 has also been expanded to more rigorously test the user interface (UI) design. R7.1 and R7.2 now evaluate how intuitive the UI is through both quantitative and qualitative metrics and have target values of no mistakes and “Strongly agree” on a Likert scale, respectively. Finally, R7.3 evaluates how quickly the device is able to elicit a response from a user while notifying them of a severe leak and has a target value of less than 10 seconds.

The constraints and their associated critical values can be seen in Table A2 in the Appendix. Justifications for the target values of C1 to C10 can also be found in the final report from BME 461 [14]. An additional constraint to limit the total size of the device (C11) was added to ensure the device fit underneath the wheelchair used for the design symposium.

3.2 MECHANICAL AND ELECTRICAL DESIGN

Various changes were implemented when transitioning from the medium- to high-fidelity prototype. One of the main changes was the downsizing of components to more successfully meet R8/C11. The newly sourced components also better satisfied R5.1 and R6/C6 regarding the noise created by the system and the overall cost of the device. The medium-fidelity prototype used electromechanical relays to control the valves and the pump. These components were large and made a loud clicking sound when triggered. Additionally, a total of 6 relays were required to control all of the required loads. Two alternatives were compared: solid-state relays and a Darlington transistor array. Solid-state relays are slightly smaller and do not make a noise when triggered. However, they are only available for AC or high-current applications. Darlington transistor arrays provide high amplification of current when provided with a lower current input signal from the Arduino to control the operation of the loads. The Darlington transistor array is significantly smaller than both relay options, is silent, and only one is required to control all of the required loads which reduces cost.

The team continued to evaluate the medium fidelity prototype to further satisfy R8. Sourcing and/or designing components with barbed fittings instead of National Pipe Taper (NPT) fittings allowed for the use of smaller components and a smaller housing. Using barbed fittings meant that the outer diameter of the tubing was the limiting factor in reducing size. The medium fidelity prototype originally used an off-the-shelf manifold with attached NPT fittings. The considered alternative was a custom manifold designed with barbed fittings and printed using a stereolithography (SLA) resin printer. A resin printer was used instead of a fused deposition modelling (FDM) printer because it chemically bonds each layer together rather than using mechanical bonds, creating a more airtight component less prone to leaks [19]. This part was also printed in various orientations to evaluate the best location for the supports to avoid inducing leaks from these impurities, and compared via bubble tests. In addition to the manifold, smaller valves were sourced. These valves use barbed fittings instead of NPT fittings and are approximately half the size, and 25% of the price of the valves used in the medium-fidelity prototype, better satisfying C11 and R6.

Multiple iterations of the housing were designed to hold the electromechanical components. The first iteration was for the medium-fidelity prototype to experiment with different component orientations. This proved to have limitations in its large size, inability to fit certain components, and inability to be FDM printed in one part. To address these limitations, CAD models of all the electromechanical components were created and used in SolidWorks Assembly to optimise component placement and fit in the next design. Particular care was given to critically examining the stresses experienced by all components in this new design as the 3D-printed barbed fittings were more delicate than the original NPT fittings. In this design, the alignment of pneumatic components was prioritised to avoid stresses caused by bent tubing. The mounting systems for all electrical components were also designed to minimise the size of the housing and to streamline the construction of the prototype. Ultimately, the size reduction of both the valves and Darlington transistor array component allowed the housing to be less than half the size of the medium-fidelity prototype, thus better satisfying R8 and C11 increasing manufacturability.

As per C1, the system must have self-sustained power. Two types of batteries were evaluated: NiMH batteries and Li-ion batteries. Li-ion batteries are known for having high energy densities, high voltage ratings, and large capacities while NiMH batteries are known to supply high current at once [20]. For this application, it is important to consider that Li-ion batteries allow for fast charging, have a low self-discharge rate, and a long lifespan [20]. However, they are relatively expensive when compared to NiMH batteries [20]. Furthermore, the chemistry in NiMH batteries is relatively safer upon fully discharging [20]. However, NiMH batteries are much less tolerant to temperature changes which may result in overheating and potentially fire, which would not satisfy C3. Additionally, NiMH batteries have a very high self-discharge rate and very slow charge time [20]. Charge time, usability, and sustainability were heavily considered when deciding between different battery options, the team evaluated the batteries based on their specifications including capacity, self-discharge rate, and output voltage. The main limitation of a Li-ion battery is the risk it poses when consistently and drastically being fully discharged to 0%. However, this is not a concern with this system as it is not expected to fully discharge under normal circumstances. This is explained in Calculation A1. The only case where the battery may be discharged to 0% is in the event of a catastrophic leak which the system is not designed to compensate for; therefore, it would warn the user before this occurs.

At the beginning of the term, the team had an initial design for the custom spool component which allowed for direct access to each quadrant of the ROHO® cushion independently. This initial design used four $\frac{1}{4}$ " NPT fittings as the pneumatic connector type which took up a lot of space in the region behind the thighs. Since it can take as little as the seams on pants to cause a pressure ulcer [21], to accommodate C2, these connectors were downsized to be $\frac{1}{8}$ " NPT fittings for the medium-fidelity prototype, then single barbed fittings for the high-fidelity prototype and finally triple barbed fittings to prevent leaks in the final design. In addition to shrinking the connector type, the edges of the spool component were rounded to further reduce the risk of contact. Additionally, since the spool component is 3D printed as two separate parts, it requires a snap to secure locking mechanism to hold it together within the enclosed channel. Several versions of the custom locking mechanism, where the number of prongs or the space between prongs varied, were 3D printed and tested to determine the ideal locking mechanism features for the project's needs. Designing the component to be tamper-proof/resistant is an important design consideration for medical devices. In this case, the ideal locking mechanism would be one that can be easily snapped together during manufacturing but something that could not be removed by the user unless excessive force was used.

The four NXP MPX5050GP pressure transducers that were used in the final prototype were chosen because they were the most cost- and size-effective option which operated accurately within the pressure range of the PressurePro system (0 to 3 psi) [22]. A calibrated OMEGA Engineering Inc. pressure gauge with 0.01 psi precision and the same setup that was described in the BME 461 final report was used to complete calibration [14]. Calibration was conducted both with and without the output filtering circuit that is recommended by the manufacturer and all trials had a coefficient of determination of 1. Since the sensor performed just as well without the output filtering circuit, it was not included in the final design to further reduce the size of the final device and satisfy C11 and R8.

An appropriate pump should have adequate airflow in the worst case conditions. Based on the requirements and constraints, the pump should be capable of delivering a volume difference from bottoming out to ideal inflation for a user of 300lbs in under 30 minutes. Reference was made to a study regarding interface pressure for SCI patients documenting the ideal internal pressures of the ROHO® cushion for users of various weights [23]. From this study, a user of 300lbs was extrapolated to have an ideal internal pressure of 0.841 psi. Applying a safety factor of 2 to accommodate for individual differences, it was concluded that the pump must have a head pressure ≥ 1.7 psi to ensure adequate inflation under high demand scenarios. The volume difference from bottom out inflation to fitted inflation for the heaviest user was estimated to be 2L. This was determined by measuring the displacement of water made by one cell at each inflation level and extrapolating the volume data for the full cushion. This corresponds to a flow rate of 133.33mL/min over 15 minutes when a safety factor of 2 is applied to the maximum bottom out time (C8). The pumps were evaluated by ensuring the reported average airflow and max head pressure were greater than 133.33mL and 1.7 psi respectively. The requirements of the device not being noisy, as well as being small and light were also considered.

3.3 ALGORITHM DESIGN

In the previous term the team selected one design concept for the algorithm which determines when to activate the pump and deflate functions based on trends in pressure. This algorithm was selected based on its superior specificity and response time to unideal pressures. Since last term, the team was able to implement the algorithm on the full system. This involved

collecting pressure data specific to each quadrant, taking averages per minute, and testing the pump actuation. The team found that a pressure sensor sampling rate of one second, averaged over a minute, generated data that did not reflect variation from small shifts but did indicate large pressure reliefs which could be filtered as outliers. In the case of a leak, the pressure of the leaky quadrant at bottom-out often caused misidentification as the user being unseated. A modification was added such that three quadrants were required to have pressures greater than 0.1 psi to determine a user was seated.

Since sensor values were found to fluctuate significantly when the pump was running, an inflation procedure was developed where the pump is paused for two seconds periodically during refill in order to sample the current pressure and determine the magnitude of error. The time that the pump is set on between the pressure samples is determined proportionally to the magnitude of error between the current and ideal pressures. The detectable pressure error of 0.1 psi took the pump approximately 40 seconds to return the lightest user to ideal pressure. To avoid overshoot, if the difference between current and ideal pressures is greater than 0.1 psi, a conservative maximum time of 30 seconds is taken between samples. A difference of 0.01 corresponds to the minimum time of 5 seconds between samples.

3.4 USER INTERFACE DESIGN AND HOUSING PLACEMENT

At the beginning of the term, the team evaluated design options for the device's UI and wheelchair attachment mechanism by conducting a user survey. This survey involved both an OT and an intended end-user to gather comprehensive feedback on the features, placement, and usability of the UI. Key design considerations emerged from the feedback, including the preferred housing body attachment location (under the wheelchair seat versus on the backrest), the specific placement if located under the seat (front versus back), the UI location (on the device housing versus on the armrest), and the inclusion of features including leak detection. The participants favoured attaching the device housing body under the wheelchair seat, particularly at the front of the seat, for better accessibility (R7.2), lower risk of tipping due to a lower center of gravity, and to reduce distraction (R5.2). Although the armrest was preferred for the UI location, a participant highlighted the variability in wheelchair configurations, as some users remove armrests altogether. This led to the development of an adjustable strap for the UI, allowing attachment to the armrest, frame, or any other suitable location. Feedback also indicated a preference for locating the power button on the device housing body, with other controls on a separate remote interface. The inclusion of a leak detection feature was unanimously appreciated, and the OT relevant functionality like the *Set New Reference* button and *Setup Mode* switch was confirmed to be easy to understand. These design considerations were crucial in meeting specific design requirements, notably making the device easily attachable (R4.1) and detachable (R4.2), ensuring the UI is easy to understand (R7.1), easy to use (R7.2), capable of promptly alerting users to detrimental leaks (R7.3), and not visually distracting (R5.2).

When creating the UI circuit, the team encountered challenges with Bluetooth connectivity between the UI remote and the housing body. Given time constraints (C5), a decision was made to use a wired connection for its straightforward reliability. A custom UI housing was then designed in SolidWorks. An assembly of the electromechanical components was created to ensure the housing lid and base fit correctly. This process involved multiple iterations of redesign and 3D printing to ensure a precise fit for all components.

4. SOCIAL, ECONOMIC, & ENVIRONMENTAL IMPACTS

The PressurePro device seeks to address the health risks and effects on quality of life incurred by the development of pressure ulcers in individuals with complete SCI. The positive social impact may be quantified by assessing the differences in Disability-Adjusted Life Years (DALY) and Quality-Adjusted Life Years (QALY) with and without the device. The PressurePro was determined to improve DALY for the user group by 59.0%, and increase QALY by 37.3%, yielding an overall improvement in health outcomes of 48.2% [18].

Using bulk pricing estimates, the cost to produce a PressurePro device is approximately \$180.45 [18]. Considering the costs of marketing and administration and assuming licensing to Permobil, and the industry-average before-tax profit of 12.5%, the proposed price of the device was calculated to be \$336.57 [18]. Taking the average cost of a pressure ulcer, lifetime chance of developing one, and lifetime cost of the PressurePro device into account, gives an average lifetime savings of \$65,321 [18]. These savings justify the proposed price and demonstrate the device's potential to reduce the economic burden on both the user group and the Canadian healthcare system.

Sustainability was an important concern throughout the process of designing and prototyping the device [18]. Rechargeable batteries were chosen over disposable ones to eliminate the need for frequent disposals of single-use components, thereby increasing energy efficiency and minimising the system's environmental impact [18]. More specifically, using an NiMH battery (as compared to a Li-ion battery) significantly decreases the lifespan of the device, thus increasing waste [20]. Incurring a slightly higher cost was determined to be worth increasing usability and sustainability. The device's ability to maintain the functionality of the ROHO® over time by encouraging leak repair rather than replacement also promotes longer use of the cushion.

5. DESIGNED SOLUTION

5.1 PNEUMATIC, MECHANICAL, AND ELECTRICAL DESIGN

The final designed solution of the physical PressurePro device can be broken down into three categories, the pneumatic, electrical, and mechanical design. A diagram showing the final design of the pneumatic system can be seen in Figure A1. in the Appendix. A custom spool component slides into the pre-existing enclosed channel of the cushion and provides independent access to each quadrant through the attachment to the barbed fittings. The optimal design features for the locking mechanism of this part were determined to be 8 prongs with 0.4 mm to 0.1mm tapered spaces between them, shown in Figure A2. Each quadrant is then attached to a shut-off valve and an NXP MPX5050GP pressure transducer through a brass barbed t-fitting. The other openings of the shut-off valves are each connected to the custom manifold part that is continuous with the air pump and another shut-off valve that can release air to the atmosphere. The selected pump has a max average flow rate of 600mL/min, and an ability to overcome a max pressure of 6.53 psi. It is compatible with the battery requirements with less than 100mA current draw and requires a 12V supply voltage.

A comprehensive circuit diagram of the device can be seen in Figure A3. in the Appendix. This system contains an Arduino Uno microcontroller which controls the output to the Darlington transistor array which allows it to control the states of the five valves and pump independently and was determined to best satisfy the team's requirements for size and noise when compared to relays. The microcontroller also receives pressure data from the pressure transducers and battery power information from the voltage sensor which it can communicate

to the UI remote through a wired serial connection. The whole system, including the valves and pump, is powered by a 12V Li-ion battery with 3000mAh capacity which is stepped down to 9V via a voltage regulator to power the Arduino Uno. The 5V source from the Arduino Uno is used to power all of the sensors.

The mechanical design of the system includes the housing body, lid, and fasteners which secure the components within the housing body. The SolidWorks Assembly of the housing body containing 3D models of the components can be seen next to an image of the fully assembled device housing in Figure A4. in the Appendix. The housing was designed to prioritise the alignment of all pneumatic components to avoid unnecessary stresses between components. Three different fastener pieces were designed to hold the solenoid valves, pump, and Arduino Uno/battery in place, shown in Figure A5. Lastly, the lid of the housing was designed with bracket-like attachments which allowed the device to be fastened under the wheelchair seat with adjustable straps that do not create any additional pressure points for the user. In addition, the UI attachment mechanism was designed using a bayonet mount and adjustable straps, shown in Figure A6., allowing it to be easily attached and detached.

5.2 ALGORITHM DESIGN

When the UI is not in use, the system will default to the state of monitoring internal pressures. Each quadrant is set to have its own ideal pressure through the UI, which is stored as a reference. Every second, pressure samples are taken from each quadrant, which are then averaged every minute. If the minute average of pressure in any quadrant deviates from the quadrant's ideal pressure beyond the acceptable threshold of ± 0.1 psi, the system will perform several checks in order to determine if this indicates unideal inflation. It first checks that there is at least 15 minutes of historical data stored for that quadrant and that the user is seated. If these conditions are met, it then calculates the linear trend of the past 15 minutes, excluding data points that are more than 1.5 standard deviations from the average of the last 15 minutes, which are classified to be outliers.

If the current data point is within ± 0.1 psi of the projected datapoint from the trendline the system triggers the refill or deflate process for that quadrant. If deflating, the exhaust valve is opened and the pressure is continuously sampled for that quadrant until the error is less than 0.01 psi from the ideal value. If inflating, the procedure outlined in Section 3.3 is executed until the acceptable error of 0.01 psi is reached. The historical data is then reset for that quadrant, and the timestamp and quadrant are stored, triggering the yellow light on the corresponding quadrant LED on the UI. If there have been more than two adjustments within the last hour, this triggers the red light and alarm for the corresponding quadrant. For all quadrants, the history of leaks is checked every minute and if the most recent adjustment has been over 24 hours ago the LED corresponding to that quadrant is set to off.

5.3 USER INTERFACE DESIGN

Using the user survey feedback, the UI circuit was developed and featured an Adafruit Feather nRF52840 board chosen for its Bluetooth functionality and pin layout, and a 3.7V 400mAh lithium polymer rechargeable battery. A 7×9cm perf board was used, as it was the minimum size capable of accommodating all components.

The final design of the UI remote is shown in Figure A7. in the Appendix. It features a *Power* LED that visually indicates the charge level, and a *Setup Mode* slide switch that unlocks all cushion quadrants - red indicates off, green indicates on. When *Setup Mode* is on, the *Inflate*, *Deflate*, and *Set New Reference* buttons are active, allowing for cushion inflation adjustments.

When an OT is fitting the cushion to a user, they will turn *Setup Mode* on, overinflate the cushion using the *Inflate* button, and then deflate the cushion using the *Deflate* button until there is an appropriate distance between the lowest bony prominence and the seat of the wheelchair. They will then hold the *Set New Reference* button for three seconds to capture the ideal pressure values in each quadrant, and lastly turn *Setup Mode* off. If both *Inflate* and *Deflate* buttons are pressed and held simultaneously for 3 seconds when *Setup Mode* is off, the pressure in each quadrant resets to its ideal setting. If a new reference is set or returned to, the four quadrant LEDs flash green and the buzzer beeps. If the user is not seated, the four quadrant LEDs flash red three times and the system does not take action. The four bottom LEDs visually indicate if a quadrant has a leak. The orientation of the quadrants is denoted by the words “FRONT” which correspond to the front of the wheelchair seat. A yellow light turns on if the system detects a small leak over the past 24 hours that can be compensated for but should be repaired by the user. A red light turns on if the system detects a significant leak that cannot be compensated for and must be repaired immediately. The buzzer turns on if there is a significant leak, which can be muted using the *Mute* button. Moreover, the battery can be recharged using the Micro USB port on the side of the remote housing, and a grommet was used to secure the remote’s wired connection. The electrical schematic for the UI components is shown in Figure A3. in the Appendix.

6. SUMMARY OF DESIGN EVALUATION AND VALIDATION

In order to evaluate R1.1, R1.2, and R2 the system's performance was evaluated for various user weights, movements, and inflation levels. Three participants of weights 105 lbs, 140 lbs, and 250 lbs were selected to represent the range of weights of users. A puncture was introduced to one quadrant of the cushion, causing the users to bottom out in 15 minutes. Each user was instructed to sit on the cushion for 20 minute trials, and data was recorded for each minute average. The response time of the system in being able to detect the leak from the moment the averages were outside the acceptable range was measured, including the time required for the pump to return the pressure. For all three users the leak was detected within a minute of the data exiting the acceptable threshold, and the pump was able to refill back to the ideal pressure within 0.9 minutes for the lightest user (Figure A8.) and 2.4 minutes for the heaviest user (Figure A9.).

The robustness of the algorithm in meeting these requirements was further assessed using real and simulated leak data. Pressure variations were recorded for expected user movements including sitting still, leaning, twisting, reaching, and wheel rotations for 10 minutes. Participants also performed a variety of stationary pressure reliefs and transfers on/off the cushion. The simulated data class made to screen algorithm concepts was used, replacing the ideal pressures with the respective ideal pressures for each participant [14]. For each participant, the standard deviation of the smaller and larger shifts, as well as the non-seated values were fed into the simulated data class and labelled as cases where the system should not adjust inflation. Linear trends of varying slopes were introduced to model leaks that reached dangerous inflation levels within 15 minutes to 24 hours, and simulations were performed to represent 48 hours for each leak type rate and user. The response time and specificity of the algorithm for each participant came extremely close to the R1.1 and R1.2 target values, for the approximate range of user weights (C4), without needing further iterations. However, verification of the leak classification was limited in that the heaviest participant was still 50lbs under the upper weight limit. Furthermore, while participants attempted to mimic the expected activities and movements of the target user group, further validation should be performed by collecting data from users who have complete SCI, as they

are more likely to have bony prominences and different levels of movement/shifts than the participants used. C8 and C4 were also evaluated by ensuring that the pump was able to deliver adequate airflow for the heaviest user. A weight was added to the heaviest participant to reach the distribution of weight for a 300lb user. It took the pump 2 minutes and 32 seconds to inflate one quadrant from bottomed out to the ideal inflation level, which is well within the desired specifications.

The physical effort required to restore the cushion to ideal inflation levels (R3) was evaluated according to the Borg Physical Exertion scale [24]. During normal operating conditions, inflation adjustment is fully automated and requires no exertion. If restored to the set reference via UI, the exertion of pressing a button can be classified as low exertion. The worst case exertion level is therefore scored at 7 [24]. To evaluate the device modularity (R4), three team members were timed during the process of attaching (R4.1) and detaching (R4.2) the entire system to and from the wheelchair. The average time required to attach the full system to the wheelchair was 102.19 seconds, falling short of the 60 second target for R4.1. During the tests, the team observed that fastening the straps demanded considerable effort, suggesting that a clip-in mechanism with permanently attached straps could offer a more efficient solution. The detachment process averaged 48.34 seconds, successfully meeting the target for R4.2.

To evaluate the effectiveness in conveying device status and ease of control (R7), the team conducted user interviews with five students. Participants were given printed device instructions at the start of the interview, simulating having instructions on the back of the remote. This forced the participant to alternatively focus on the instructions and the UI, as they were not permitted to look at both at the same time. They also watched a video demonstrating how an OT fits a ROHO® cushion to a patient for contextual understanding. The interview commenced with the prompt, "As an OT fitting a cushion, which UI features would you use and in what order?" This approach revealed a knowledge gap, as participants lacked the OT's expertise, complicating their understanding and interaction with the UI. Participants were then shown a UI remote displaying a lit yellow light and asked to interpret its meaning and identify the corresponding cushion quadrant. This task was repeated with a red light, including an additional question on how to silence the alarm. The participant errors made during these tasks were noted to evaluate the clarity of UI notifications (R7.1), with an average error rate of two mistakes per participant. These results did not meet the target value of R7.1, likely due to insufficient explanation provided to participants during the interviews and the fact that interviews were not conducted on the targeted user group. Participants also rated the device's ease of use (R7.2) and visual distraction (R5.2) on a Likert scale from 1 (Strongly Disagree) to 5 (Strongly Agree). The prompt "The device is intuitive and easy to use" received an average score of 4.25/5, indicating "Agree" on the Likert scale. Similarly, the prompt "The device is not visually distracting" received an average score of 4/5, indicating "Agree" on the Likert scale. These results fell short of the desired "Strongly Agree" benchmark for R7.2 and R5.2. To evaluate the duration of the response from the user when alerted to a detrimental leak (R7.3), the red light and buzzer were turned on without warning during participant interviews. The team recorded the time taken for participants to identify and respond to this alert. On average, participants reacted within 1.4 seconds which satisfied R7.3.

R9 states that the battery should maintain power for 16 hours. The system uses 85.95% of the battery's power in the worst case scenario over 16 hours (Calculation A1). If the battery were to supply a consistent 12V output throughout its discharging cycle, this would satisfy R9.

However, as shown in Figure A10., the output voltage drops as the battery discharges. The data was collected from a circuit containing an Arduino, a voltage sensor, and the battery. The battery was charged to 100% and then discharged by various devices with readings taken every 10 minutes. The dotted lines on Figure A10. indicate the voltage corresponding to each LED battery life indicator. The solenoid valves and pump have a small range where they will function successfully outside of 12V but this range is not documented in their specification sheets. During testing, it was noted that the valves stop working when 3/5 indicator lights are on, this equates to 11V which occurs at 60% of the battery's total charge. As such, the current battery circuit does not adequately satisfy R9 and fails C1.

The noise of the device (R5.1) was tested by performing multiple trials of the worst-case scenario in which the pump is experiencing 4 psi of pressure. The maximum additional noise recorded was 24.7dB, sufficiently less than the target value of 30dB. Evaluating R6, the cost to manufacture one device was estimated to be \$180.45 which increases the costs of the device by 25.8%. This is less than the target value, satisfying R6. C6 was also satisfied as the total project cost was \$1300 and the budget was \$4000. Additionally, the system was measured using a scale and weighed 3.6 lbs. The target value was < 4 lbs and the critical value is \leq 50 lbs, thus satisfying R8 and C9.

C2 states that the device must not increase the risk of pressure ulcers in other areas. The device is attached underneath the chair and does not contact the user. The spool component is the only part that was added directly to the ROHO® Cushion. The original spool valve that comes with the cushion protrudes an additional 15.5mm on either side of the enclosed channel. The custom designed spool component sticks out 15.0mm on either side and can, therefore, be expected to not introduce new pressure points. C3 was considered while sourcing components; all electromechanical components are rated for 0-30°C as specified by the constraint. C7 states that the device must be fluid-resistant, and the current prototype fails this constraint as the lid is not currently sealed. The final product would have a hermetically sealed housing and would hypothetically pass this constraint as per the International Protection Rating IP44. C10 states that the device must not introduce leaks to the system. This was verified by conducting a bubble test; no leaks were introduced, so the constraint was satisfied. C11 states that the device must fit under the wheelchair (<13"x8"x4"). The total volume of the housing body is 8.46"x5.91"x3.11" which satisfies this constraint.

A summary of the results and scores assigned to each non-functional requirement can be seen in Table A3. A summary of the results assigned to each constraint can be seen in Table A4.

7. DESIGN SAFETY AND REGULATIONS

A medical device is defined by both the Food and Drug Administration (FDA) and Health Canada as an implement that is involved in “prevention of disease” and which “affects the structure [and] function of the body” [25]. The moderate risk posed to the user due to the active pressure-modifying components categorises it as Class 2 according to both authorities. In Canada, this classification necessitates a medical device licence, manufacturing quality system certification and conformity declaration in bringing the device to market. To achieve these certifications, relevant medical device standards by the International Organization for Standardization (ISO) and International Electrotechnical Commission (IEC) were identified. The electrical components were designed with IEC 60601-1 and 60601-2, which outlines general electrical safety practices. The team ensured that the chosen battery was placed in a portable sealed secondary cell according to IEC 62133. For the pressure system components,

the ISO 4414 pneumatic safety requirements were implemented by ensuring that a pump with a low pressure limit (6.53 psi) was chosen, testing all connections for leaks before system assembly, and including pressure sensors to monitor pressure levels. IEC 62304, which outlines life-cycle processes for medical device software, was followed by ensuring traceability through version control and performing thorough verification testing on the algorithm's functionality (Section 6). ISO 14971, which outlines risk management processes for medical devices, was kept in mind throughout the design and prototyping process. The team made an effort to control risks that were identified; for instance, in response to the risk of a short circuit, a fuse was installed.

8. LIMITATIONS OF DESIGNED SOLUTION

One of the main limitations identified during the V&V testing was the inconsistent voltage supplied to the system by the battery. Another limitation is that the custom spool component and manifold were not designed for traditional manufacturing methods and additive manufacturing would be required instead. Due to their delicate nature, it would also be ideal for these parts to be manufactured out of aluminium for its durability and lightweight properties. While creating these parts using aluminium 3D printing is a viable option, it tends to be more expensive and slower than traditional metal manufacturing techniques such as casting or machining. A comprehensive cost-benefit analysis would need to be conducted to determine whether aluminium 3D printing or alternative manufacturing techniques would be more suitable for these parts. In the event traditional techniques are favoured, it would necessitate redesigning the parts as outlined in the recommendations section below.

The wired connection between the UI remote and the main system unit posed a limitation to convenience and safety as it could easily tangle in the wheels. The shielded cable was also bulky, adding clutter where a user may already have several attachments. Moreover, the UI remote itself was bulky due to the large size of the Adafruit Feather nRF52840 board and other electrical components. The Arduino Uno, intended for prototyping, has low SRAM and flash memory, which limits algorithm complexity and available data storage in classifying patterns such as the user being seated.

Since the high-fidelity prototype was designed to have accessible ports for the purpose of demos at the design symposium, the prototype was not perfectly sealed off from the environment and did not satisfy C7. This limitation could be addressed using some of the strategies suggested in the section below.

9. CONCLUSIONS AND RECOMMENDATIONS

Overall, the designed solution met the target value for requirements R4.2, R5.1, R6, R7.3, and R8 and performed well for all other requirements except R9. Additionally, the device satisfied all constraints except for C1 and C7. The following recommendations could be implemented in the future to improve upon the design of the system to better satisfy the engineering specifications.

A few changes should be implemented to improve the limitations of the battery. As shown in Figure A10, the battery's output voltage decreases by 0.5V for every 20% decrease in battery power. There are two options to maintain a consistent 12V output. One option is to implement a boost convert that maintains voltage by pulling more current from the battery.

The alternative is to source a higher voltage battery that can be stepped down using either a buck converter or a linear dropout regulator which releases excess energy as heat. To evaluate these alternatives, cost and battery life would need to be compared (R6 and R9).

If traditional manufacturing techniques were favoured to mass produce the custom spool component and manifold, both parts would require design adjustments to avoid compromising the internal airflow channels. One method could involve separating the parts at channel intersection points so that they can be manufactured separately, screwed together, and sealed using anaerobic thread sealants similar to the ROHO® valve design. Additionally, to address the limitations related to the fluid resistance of the housing, the interface between the lid and the housing body could be redesigned to incorporate a sealing mechanism such as a rubber gasket or an O-ring. Additionally, secondary sealing measures such as epoxy seals or silicone caulking could be added around joints and openings to further enhance fluid resistance and seal any potential ingress points. V&V testing showed that R4.1 was not adequately satisfied. To improve the attachment mechanism, the design could be modified such that the device clips into a separate part which is affixed to the wheelchair via straps to increase the ease of handling the device. To enhance safety, fail-safes like bottom-out sensors and mechanical relief valves should also be added to alert users of unsafe inflation levels and prevent unnoticed cushion over- or under-inflation.

A custom PCB with an nRF52840 embedded chip may be used for the main system unit. This chip meets the electrical needs of the existing system; it can output the 5V necessary to power the pressure transducers, and has many pins that can be configured as GPIOs to accept and transmit signals [26]. It has built-in Bluetooth Low Energy (BLE) capability [26] that the current Arduino Uno does not have, allowing for increased flexibility in connecting to a remote or mobile app. This chip also has larger SRAM and flash memory, as well as increased processing power [26], allowing for development of more complex data processing algorithms. While the algorithm was sufficiently robust for the participants tested, more work should be done in the method to determine if the user is seated, as even one mis-identified case can lead to dangerous inflation levels. This custom PCB would also minimize the size of the remote, making it easier to handle (R7.2) and less visually distracting (R5.2). A render of an updated, smaller remote is shown in Figure A7. A mobile application could also be a viable option as an alternative remote. This would allow users with diverse needs to leverage the built-in accessibility settings on their phones such as voice commands, screen readers, and alternative input methods.

10. ACKNOWLEDGEMENTS

Our team would like to acknowledge the support that we have received from our capstone advisor, Professor Jenny Howcroft, who facilitated our engagement with stakeholders via the Stakeholder Café and has provided useful direction throughout the project. Our gratitude also extends to Permobil for their generous cushion donation as well as funding we received through the Baylis Medical Capstone Design Award and the Canadian Posture & Seating Centre Scholarship. Special thanks to Alex Magdanz, Calvin Young, and Bryan Tripp for their expert guidance and mentorship throughout this project.

11. REFERENCES

- [1] C. H. Lyder, “Pressure ulcer prevention and management,” *Jama*, vol. 289, no. 2, pp. 223–226, 2003.
- [2] T. Kasai, T. Isayama, and M. Sekido, “Squamous cell carcinoma arising from an ischial pressure ulcer initially suspected to be necrotizing soft tissue infection: A case report,” *Journal of Tissue Viability*, vol. 30, no. 4, pp. 621–625, 2021.
- [3] Z. E. Moore, M. T. van Etten, and J. C. Dumville, “Bed rest for pressure ulcer healing in wheelchair users,” *Cochrane Database of Systematic Reviews*, no. 10, 2016.
- [4] A. O. Iyun, A. O. Malomo, O. M. Oluwatosin, S. A. Ademola, and M. T. Shokunbi, “Pattern of presentation of pressure ulcers in traumatic spinal cord injured patients in university college hospital, ibadan,” *International wound journal*, vol. 9, no. 2, pp. 206–213, 2012.
- [5] D. Fogelberg, M. Atkins, E. Blanche, M. Carlson, and F. Clark, “Decisions and dilemmas in everyday life: Daily use of wheelchairs by individuals with spinal cord injury and the impact on pressure ulcer risk,” *Topics in spinal cord injury rehabilitation*, vol. 15, no. 2, pp. 16–32, 2009.
- [6] B. C. Chan, N. Nanwa, N. Mittmann, D. Bryant, P. C. Coyte, and P. E. Houghton, “The average cost of pressure ulcer management in a community dwelling spinal cord injury population,” *International wound journal*, vol. 10, no. 4, pp. 431–440, 2013.
- [7] S. Pritchard, H. Cardoza, and S. Stupalo, “Biomedical Stakeholder Cafe”, In-Person Meeting (October 4, 2023).
- [8] C. He and P. Shi, “Interface pressure reduction effects of wheelchair cushions in individuals with spinal cord injury: a rapid review,” *Disability and Rehabilitation*, vol. 44, no. 6, pp. 826–833, 2022.
- [9] M. Trewartha and K. Stiller, “Comparison of the pressure redistribution qualities of two air-filled wheelchair cushions for people with spinal cord injuries,” *Australian occupational therapy journal*, vol. 58, no. 4, pp. 287–292, 2011.
- [10] H. K. Yuen and D. Garrett, “Comparison of three wheelchair cushions for effectiveness of pressure relief,” *The American Journal of Occupational Therapy*, vol. 55, no. 4, pp. 470–475, 2001.
- [11] J. Howcroft, E. Boulanger, and I. Ahmed-Fazal, “Biomedical Stakeholder Cafe”, In-Person Meeting (October 3, 2023).
- [12] “MAUDE - Manufacturer and User Facility Device experience,” [accessdata.fda.gov](https://accessdata.fda.gov/scripts/cdrh/cfdocs/cfMAUDE/results.cfm), [Online], Available: <https://www.accessdata.fda.gov/scripts/cdrh/cfdocs/cfMAUDE/results.cfm> (accessed Dec. 2, 2023).

- [13] FDA, "Maude adverse event report: ROHO, Inc.. ROHO® quadro select® high profile® cushion; wheelchair cushion," U.S. Food & Drug Administration, [Online], Available: https://www.accessdata.fda.gov/scripts/cdrh/cfdocs/cfmaude/detail.cfm?mdrfoi_id=17720290&pc=KIC&device_sequence_no=1&fbclid=IwAR21U81hrDNswQgHKGRoIxGYwspg-ZUnp_UgKcv332IKuXMN70R0GMZb-U (accessed Nov. 9, 2023).
- [14] S. Stupalo, M. Lacoste, I. Ahmed-Fazal, H. Cardoza, and E. Boulanger, "Automated Air-Cushion Pressure Corrections for Manual Wheelchair Users with a Complete Spinal Cord Injury," BME461 Class Deliverable, Dept. Biomed. Eng., Univ. of Waterloo, Waterloo, Canada, Dec. 05, 2023.
- [15] K. West, "Quokka large vertical mobility bag : Quick release mount," Mobility, [Online], Available: <https://www.mobility-aids.com/quokka-large-vertical-mobility-bag.html> (accessed Feb. 7, 2024).
- [16] "Wheelchair bag- handy bag under Bag Installation," YouTube, [Online], Available: <https://www.youtube.com/watch?v=xhOyLKTq2oU> (accessed Feb. 8, 2024).
- [17] Amazon.com: Samdew Wheelchair Backpack, wheelchair bag to hang on back, with Thermal Insulation Pockets for Medicine & Lunch Box, functional wheelchair accessories with crutches pockets, bag only, patented design : Health & Household, [Online], Available: <https://www.amazon.com/Wheelchair-Backpack-Insulation-Functional-Accessories/dp/B09PYDTJ94> (accessed Feb. 7, 2024).
- [18] S. Stupalo, M. Lacoste, I. Ahmed-Fazal, H. Cardoza, and E. Boulanger, "BME 462 Engineering Economics Assignment," BME462 Class Deliverable, Dept. Biomed. Eng., Univ. of Waterloo, Waterloo, Canada, Feb. 16, 2024.
- [19] A. Kafle, E. Luis, R. Silwal, H. M. Pan, P. L. Shrestha, and A. K. Bastola, "3D/4D Printing of polymers: Fused deposition modelling (FDM), selective laser sintering (SLS), and stereolithography (SLA)," Polymers, vol. 13, no. 18, p. 3101, 2021.
- [20] Chengjoseph, "Comparing li-ion vs Ni-MH Battery which is Better Choice," Tycorun Batteries, [Online], Available: <https://www.tycorun.com/blogs/news/comparing-li-ion-vs-ni-mh-battery-which-is-better-choice> (accessed Feb. 20, 2024).
- [21] "Common Noise Levels: How Loud is Too Loud?" International Noise Awareness Day, [Online], Available: <https://noiseawareness.org/info-center/common-noise-levels/> (accessed Feb. 20, 2024).
- [22] "Freescale Semiconductor, 'MPXx5050 Series Integrated Silicon Pressure Sensor On-Chip Signal Conditioned, Temperature Compensated and Calibrated Datasheet MPX5050 Rev 11,' Freescale Semiconductor, Inc., Dec. 2010. Available, <https://den.uwaterloo.ca/datasheet/553D.pdf>

- [23] K. Hamanami, A. Tokuhirb, and H. Inouea, "Finding the Optimal Setting of Inflated Air Pressure for a Multi-cell Air Cushion for Wheelchair Patients with Spinal Cord Injury," *Acta Med. Okayama*, vol. 58, no. 1, pp. 37-44, 2004.
- [24] N. Williams, "The Borg rating of perceived exertion (RPE) scale," OUP Academic, [Online], Available: <https://academic.oup.com/occmed/article/67/5/404/3975235> (accessed Mar 1, 2024).
- [25] J. Howcroft. BME 362. Class Lecture, Medical Device Regulations; "Wk1 - Thursday - Course Introduction. Capstone Project. Medical Devices," Dept. of Systems Design Engineering, University of Waterloo, Waterloo, Canada, September 7, 2022.
- [26] "nRF52840," Nordic Semiconductor, [Online], Available: <https://www.nordicsemi.com/Products/nRF52840> (accessed Apr. 7, 2024).
- [27] J. Howcroft, E. Boulanger, and I. Ahmed-Fazal, "Biomedical Stakeholder Cafe", In-Person Meeting (October 3, 2023).
- [28] D. Fogelberg, M. Atkins, E. Blanche, M. Carlson, and F. Clark, "Decisions and dilemmas in everyday life: Daily use of wheelchairs by individuals with spinal cord injury and the impact on pressure ulcer risk," Topics in Spinal Cord Injury Rehabilitation, vol. 15, no. 2, pp. 16–32, 2009. doi:10.1310/sci1502-16
- [29] Permobil, "ROHO® DRY FLOATATION® Cushions Operation Manual," October 2022. [Online]. Available: <https://permobilwebcdn.azureedge.net/media/g50nhaaq/dry-floatation-cushions-manual-t20200-2022-10-17.pdf> (accessed Dec 2, 2023).
- [30] Environment and Climate Change Canada, "Temperature change in canada canadian environmental sustainability indicators," 2023. [Online]. Available: <https://www.canada.ca/content/dam/eccc/documents/pdf/cesindicators/temperature-change/2023/temperature-change-en-2023.pdf> (accessed Dec. 3, 2023)
- [31] Y. Fang, L. Morse, N. Nguyen, N. Tsantes, and K. Troy, "Anthropometric and biomechanical characteristics of body segments in persons with spinal cord injury," Journal of biomechanics, vol. 55, pp. 11–17, 2017.
- [32] Permobil, "Manual wheelchair guide." [Online]. Available: <https://hub.permobil.com/manual-wheelchair-guide> (accessed Dec. 2, 2023)
- [33] I. E. Commission et al., "IEC 60529: degrees of protection provided by enclosures (IP code)," National Electrical Manufacturers Association: Rosslyn, VA, USA, 2004.
- [34] Harsh Environment Connectors and Wire harnessing, "IP Rating Chart." [Online]. Available: <https://www.dsmt.com/resources/ip-rating-chart/> (accessed Feb. 3, 2024)
- [35] "Pressure ulcers symptoms and treatments," NHS inform, [Online], Available: <https://www.nhsinform.scot/illnesses-and-conditions/skin-hair-and-nails/pressure-ulcers/#causes-of-pressure-ulcers> (accessed Dec. 3, 2023).

[36] “NIOSH Lifting Equation - Assessing Relevant Handling Factor,” Canadian Centre for Occupational Health and Safety, [Online], Available: <https://www.ccohs.ca/oshanswers/ergonomics/niosh/assessing.pdf> (accessed Oct. 5, 2023).

[37] “Leak rates explained,” Clippard, [Online], Available: <https://www.clippard.com/cms/wiki/leak-rates-explained> (accessed Dec. 3, 2023).

12. APPENDIX

Table A1. Non-Functional Requirements and Associated Target Values [Source: SS, 2024].

Non-Functional Requirement	Target Value
R1	Should replace the need for the user to perform daily pressure checks
R1.1	Should rapidly detect unsafe inflation levels
R1.2	Should not actuate when the cushion is at the appropriate inflation level
R2	Should maintain the inflation level of each quadrant that has been determined by an occupational therapist
R3	Should minimize the physical effort required to correct non-ideal pressure levels
R4	Should be modular from the wheelchair
R4.1	Should be easily attachable to the wheelchair
R4.2	Should be easily detachable from the wheelchair
R5	Should not be distracting to the user during their daily activities
R5.1	Should be quiet
R5.2	Should not be visually distracting
R6	Should minimise the increase in cost
R7	User interface should be effective at indicating the status of the device to the user and easy for them to control
R7.1	User interface notifications should be easy to understand
R7.2	User interface controls should be easy to use
R7.3	User interface should promptly alert the user to a detrimental leak (red light and buzzer) by eliciting a quick response from the user
R8	Should be lightweight
R9	Should sustain battery power for prolonged periods

Table A2. Constraints and Associated Critical Values [Source: SS, 2024].

Constraint	Critical Value(s)
C1	≥ 10 hours [28]
C2	0 points of contact
C3	0-30 °C [29, 30]
C4	100 - 300 lbs [31, 32]
C5	March 21st, 2024
C6	\$4000
C7	IP44 [33, 34]
C8	≤ 30 minutes [35]
C9	≤ 50 lbs [36]
C10	< 0.0002 cm ³ per minute [37]
C11	(L×W×H) < 13"×8"×4"

Table A3. Verification and Validation Results for the Non-Functional Requirements [Source: SS, 2024].

Req.	Metric (unit)	Scoring Scale					Result	Score
		0	25	50	75	100		
R1.1	Time (minutes)	> 30	20 - 30	10 - 20	5 - 10	< 5	5.85	75
R1.2	Specificity (%)	Score is the direct specificity %					98.5	98.5
R2	Pressure difference from reference (psi)	> ± 0.4	± 0.3 to ± 0.4	± 0.2 to ± 0.3	± 0.1 to ± 0.2	< ± 0.1	0.15	75
R3	Borg RPE scale	> 12	11 - 12	9 - 10	7 - 8	6	7	75
R4.1	Time (seconds)	> 150	120 - 150	90 - 120	60 - 90	< 60	102.19	50
R4.2	Time (seconds)	> 150	120 - 150	90 - 120	60 - 90	< 60	48.34	100
R5.1	Sound intensity (dB)	> 60	50 - 60	40 - 50	30 - 40	< 30	24.7	100
R5.2	Subjective evaluation (Likert Scale)	Scored based on the average response to the prompt: “The device is not visually distracting.”					Agree	75
		Strongly Disagree	Disagree	Neutral	Agree	Strongly Agree		
R6	Cost increase (%)	> 80	70 - 80	60 - 70	48.15 - 60	≤ 48.15	25.8	100
R7.1	Number of mistakes	> 4	3 - 4	2 - 3	1 - 2	< 1	2	75
R7.2	Subjective evaluation (Likert Scale)	Scored based on the average response to the prompt: “The device is intuitive and easy to use.”					Agree	75
		Strongly Disagree	Disagree	Neutral	Agree	Strongly Agree		
R7.3	Time (s)	> 120	60 - 120	20 - 60	10 - 20	< 10	1.3	100
R8	Weight (lbs)	> 50	25 - 50	10 - 25	4 - 10	< 4	3.6	100
R9	Time (hours)	< 10	10 - 12	12 - 14	14 - 16	> 16	< 16	0

Table A4. Verification and Validation Results for the Constraints [Source: SS, 2024].

Constraint	Critical Value(s)	Result	Pass/Fail
C1	≥ 10 hours	< 10 hours	Fail
C2	0 points of contact	0 points of contact	Pass
C3	0-30 °C	Functional	Pass
C4	100 - 300 lbs	Functional	Pass
C5	March 21st, 2024	March 17th, 2024	Pass
C6	\$4000	\$1360.52	Pass
C7	IP44	N/A	Fail
C8	≤ 30 minutes	17.5 minutes	Pass
C9	≤ 50 lbs	3.6 lbs	Pass
C10	$< 0.0002 \text{ cm}^3$ per minute	0 cm^3 per minute	Pass
C11	$(L \times W \times H) < 13'' \times 8'' \times 4''$	$8.46'' \times 5.91'' \times 3.11''$	Pass

Table A5. Current Draw from System's Electrical Components [Source: EB, 2024].

Component	Current Draw (mA)	Quantity	Total Current Draw (mA)
Solenoid valve	220	5	1100
Pump	100	1	100
Pressure transducer	10	4	40
Arduino	80	1	80

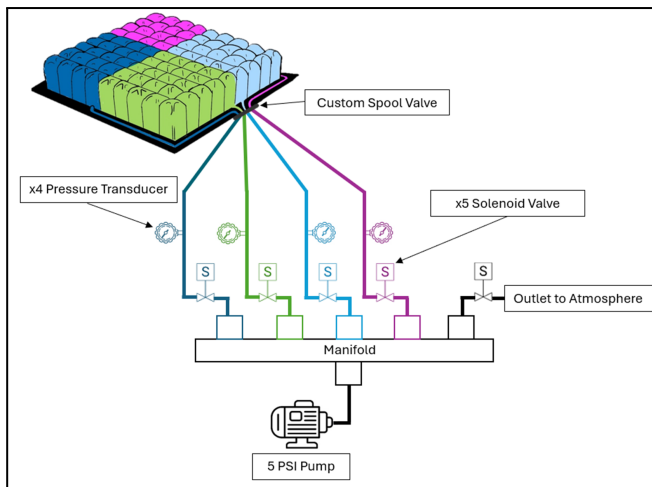


Figure A1. Final Design of the Pneumatic System [Source: SS, 2024].

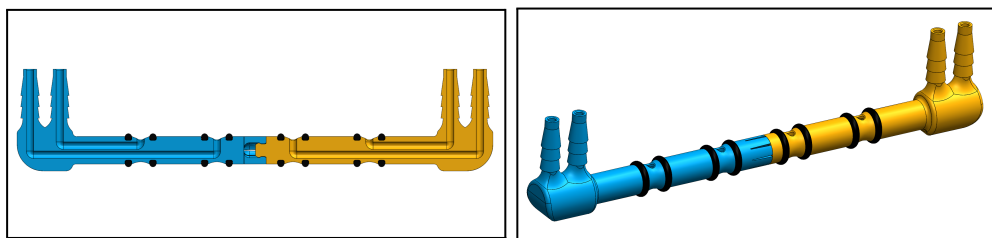


Figure A2. Final Design of Custom Spool Component [Source: SS, 2024].

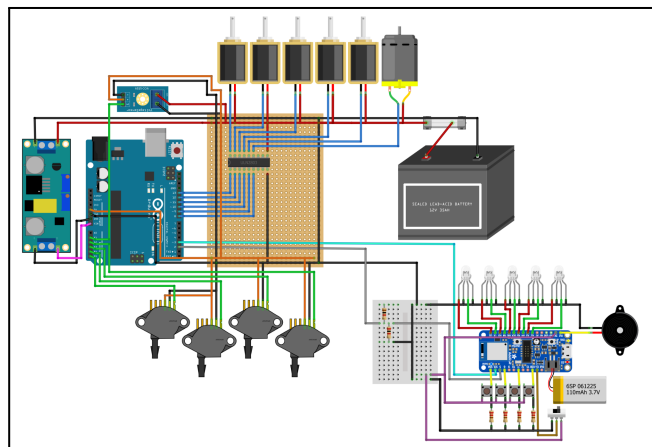


Figure A3. Comprehensive Circuit Design [Source: SS, 2024].

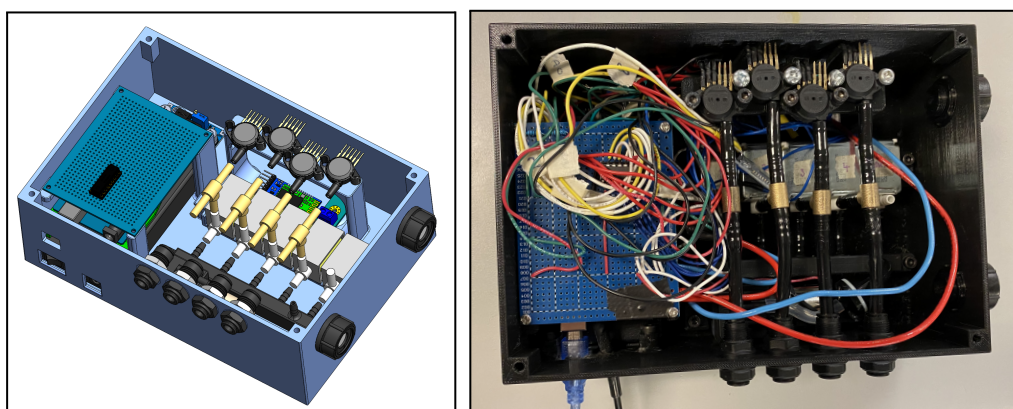


Figure A4. Assembled Device Housing [Source: SS, 2024].

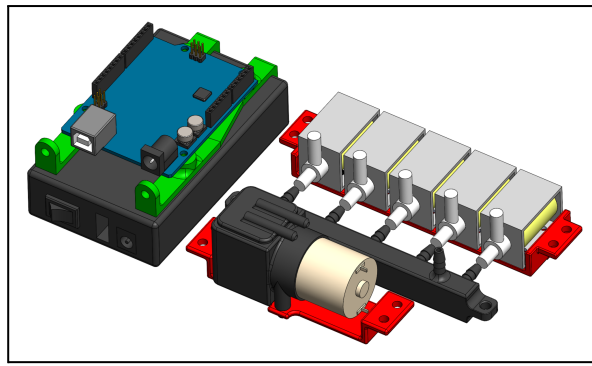


Figure A5. Three Fasteners (green and red parts) Designed to Hold the Valves, Pump, and Arduino Uno/Battery [Source: SS, 2024].

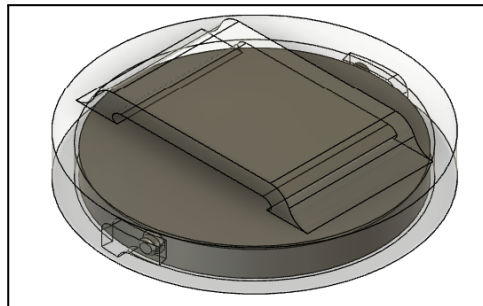


Figure A6. UI Attachment Mechanism Designed Using a Bayonet Mount [Source: EB, 2024].

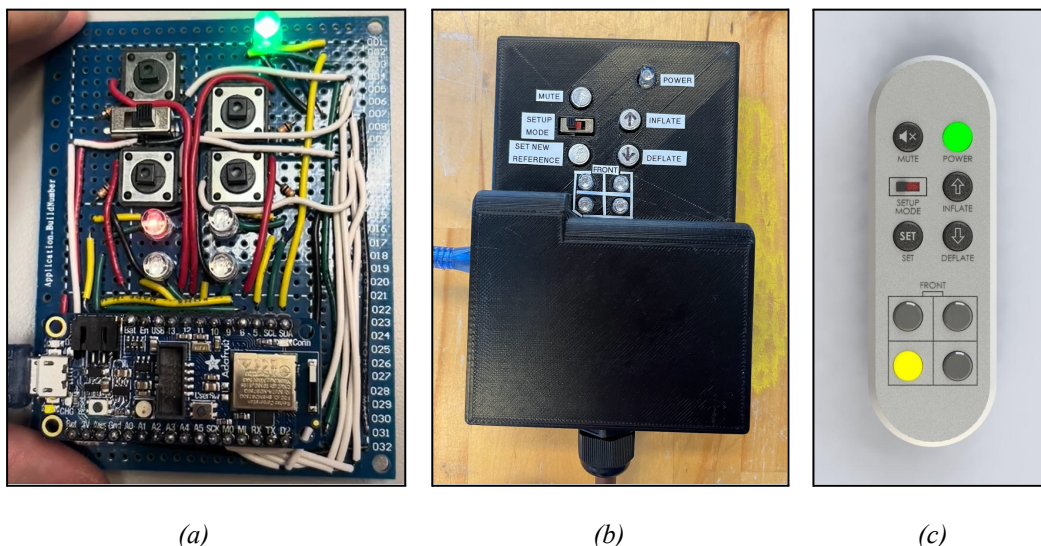


Figure A7. UI Circuit (a), Final UI Remote Assembly (b), and Rendered Model of an Improved UI Design . [Source: HC, 2024].

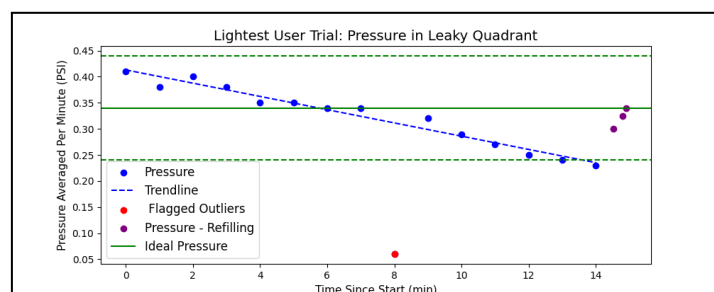


Figure A8. Quadrant Pressure Data for Leak Trial for Lightest Participant (105 lbs) [Source: IAF, 2024]

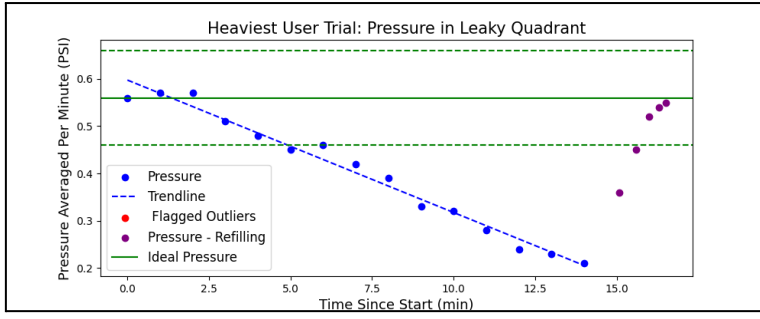


Figure A9. Quadrant Pressure Data for Leak Trial for Heaviest Participant (250lbs) [Source: IAF, 2024]

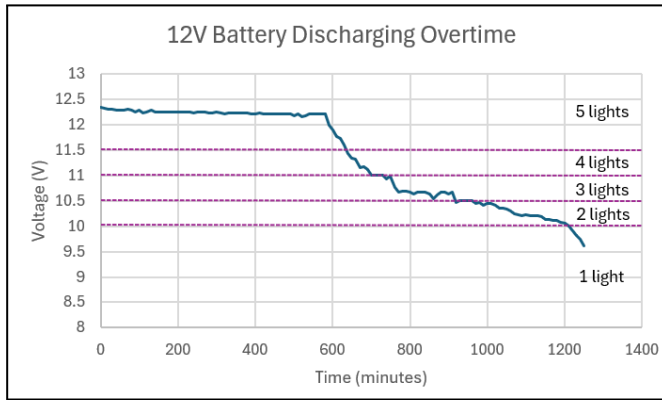


Figure A10. Voltage Drop and Battery Life As A Function of Time [Source: EB, 2024]

Calculation A1. Battery Life Calculation

Worst case scenario: a leak in each quadrant requiring filling once per hour, any leak larger than this is considered catastrophic and should be repaired by the user immediately

Maximum allowed time to be outside of ideal inflation level: 30 minutes

Requirement for battery life: 16 hours

Component current draw: Refer to Table A5.

The pressure transducers and Arduino are drawing current for the whole 16 hours:

$$(40\text{mA} + 80\text{mA}) \times 16\text{h} = 1920\text{mAh}$$

The pump will run 16 times for a maximum of 2 minutes 32 seconds (0.042 hours) each time based on the worst case scenario for inflation time from a bottomed out state:

$$100\text{mA} \times (16 \times 0.042\text{h}) = 67.2\text{mAh}$$

Four solenoid valves will be open for a maximum of 16 times for 2 minutes 32 seconds (0.042 hours):

$$880\text{mA} \times (16 \times 0.042\text{h}) = 591.36\text{mA}$$

Total current draw over 16 hours:

$$1920\text{mAh} + 67.2\text{mAh} + 591.36\text{mA} = 2578.56\text{mAh}$$

% of Total Battery Usage:

$$(2578.56\text{mAh}/3000\text{mAh}) \times 100 = 85.95\%$$

The battery has a 3000mAh capacity, using the information from the components' specification sheets, the system would draw 2578.56mAh in the worst-case scenario. This equates to 85.95% of the battery's power over 16 hours.

BME 462 Individual Contribution Statement and Reflection

PressurePro / Team 17

Sophie Stupalo

20827311

BME 462: Biomedical Engineering Design Workshop 3

Professor Bryan Tripp

April 8th, 2023

Part One: Personal Contributions

At the beginning of the term my role was Lead Electrical Designer for the project. In this role I was responsible for the design and implementation of the device's electrical circuit, and I accomplished all of my assigned tasks. As the term progressed, my skills naturally led me to take on more mechanical design work in addition to the electrical design. My key contributions to the project over the course of the term can be seen in Table 1 below and the evidence for each contribution can be found in my Engineering Logbook on the log numbers indicated in the brackets e.g., (124).

Table 1. Documentation of Personal Contributions throughout the 4B Term.

Contribution	Description of Contribution & Outcomes
<i>Custom Spool Component</i>	
Design and 3D modelling (73)	Building off of the original design of the spool valve in the ROHO cushion, I created a CAD model of a custom spool component which allowed us to access each quadrant of the cushion independently.
Iterated on the blind snap to secure lock mechanism (88)	I modelled and 3D printed several different versions of the custom locking mechanism for the spool component to test different designs where the number of prongs or the space between prongs varied. This allowed me to determine the ideal locking mechanism features for the project's needs.
Iterated on the connector type (73, 88, 103)	As the term progressed, I changed the pneumatic connector type on the spool component from 1/4" NPT fittings to 1/8" NPT fittings to single barb fittings and finally to triple barb fittings to minimize the size of the component and to prevent leaks.
<i>Medium-Fidelity Prototype (MFP; not including UI)</i>	
Electrical circuit design (49, 52, 53)	I consulted component datasheets and received advice from Calvin Young to design a comprehensive diagram for the control circuit with Fritzing.
Pneumatic and electrical system assembly (95, 96)	I manufactured parts for and assembled the pneumatic system, constructed the electrical system, and created a temporary housing which allowed the team to use the device for algorithm testing and further iterative design.
<i>High-Fidelity Prototype (HFP; not including UI, unless specified)</i>	
Sensor calibration (89)	I setup and tested the pneumatic and electrical systems required to calibrate the final pressure sensors. During this session, I also verified that the sensors were sufficiently accurate without the addition of the recommended output filtering circuit which allowed us to reduce the size of the final design.
Sourced UI & device components (99, 102)	I sourced upgraded components for the UI and the device. Notably, I sourced new valves that draw less current (250mA), which allowed us to use a Darlington transistor array to control the state of the valves and pump. This change significantly reduced the size of the HFP compared to the MFP.
Electrical design (93, 94, 108, 135)	I consulted component datasheets to update the design of the circuit to include the new components and I designed a comprehensive diagram for the control circuit and UI all using Fritzing.
Manifold design (103, 108, 118)	I 3D modelled a manifold component and iterated on the design for an optimised fit in the final housing. 3D printing this part significantly reduced the weight of the HFP compared to the MFP.
Housing design (110, 111, 118, 119)	I iteratively designed a housing for the device by optimizing component placement, and by aligning all of the pneumatic components to avoid the need to bend any of the tubing. This achieved an overall size reduction of the housing by 50%.
GUI development for testing (123)	I developed a GUI using Processing4 and Arduino that allowed each valve and the pump to be independently controlled with buttons on a touch screen while displaying real-time output from the sensors. This allowed us to both test and demo the device.
WATiMake 3D Printing (119, 120, 122, 126)	I completed the LEARN training modules and in-person training sessions to be able to use the Form 3+ (SLA) and Raise 3D E2 (FDM) printers. I used the SLA printer to print the spool component and manifolds (to ensure pneumatic integrity) and I used the FDM printers to print the housing and all of the fastener parts.
Pneumatic system assembly (120, 124)	I assembled the pneumatic system and organized all of the components into the housing box as planned in the SolidWorks assembly. Throughout the process, I performed bubble tests at every connection point to verify that no leaks were present in the system.
Electrical system soldering (120, 124, 134)	I planned and soldered components to the Arduino directly or to the perf board as specified by the circuit diagram. I verified the functionality of this final prototype which was demonstrated at the design symposium and used for verification and validation testing.

Part Two: Specific Technical Contribution

Nature of Contribution:

During BME 462, my key technical engineering contribution was designing, manufacturing, and assembling the high-fidelity prototype of the device not including the user interface (UI) portion, the wheelchair attachment mechanism, or the algorithm. This involved designing and 3D printing the device housing and retaining brackets, designing and constructing the electrical system, and assembling the pneumatic system. These tasks required many of the applied science and design principles that I learned throughout my undergraduate degree and during co-op work terms. The process that I followed to design the device housing involved the appropriate use of engineering tools, specifically, the use of SolidWorks Assembly. For this task, I drew heavily on the skills that I acquired during my final co-op term while developing medical devices and moulding tool assemblies. I also used principles from BME 281 to critically examine the stresses experienced by all of the components in the first design iteration. This influenced me to design a second version of the housing where I prioritized aligning all of the pneumatic components to avoid stresses caused by bent tubing. I also carefully planned out mounting systems for all of the electrical components to minimize the size of the housing and to streamline the construction of the prototype. By thoroughly reviewing datasheets, speaking with Calvin Young, and using principles from BME 294 I developed a comprehensive diagram for the control circuit in Fritzing that included a Darlington transistor array which allowed for the coordination of the states of all five valves and the pump independently. Once the detailed design was completed, I spent a few days constructing the prototype which began by 3D printing the housing, manifold, and retaining brackets. I then assembled the pneumatic system with careful attention to the conformity of the fit of every component with the detailed design in the SolidWorks assembly file. Once all of the parts were fastened down, I carefully soldered all of the electrical components to the Arduino or perf board as specified by the circuit diagram.

Impact on the Design:

My contribution to the creation of the high-fidelity prototype of the device had a substantial impact on the overall designed solution, particularly its functionality, usability, and presentation. The design and construction of the device housing, electrical system, and pneumatic system resulted in a sophisticated prototype that allowed for effective testing and demonstration. The compact and sleek housing design not only facilitated discreet mounting below the wheelchair but also improved the device's overall aesthetics, making it visually appealing and easy to showcase during the symposium. Ultimately, this contribution provided the necessary physical prototype for the algorithm sub-team to conduct crucial testing, significantly advancing the progress of the project and enhancing its potential for real-world application.

Verification/Evaluation:

Prior to printing the device housing, I verified that all of the components would fit as expected by using datasheets to model each part in SolidWorks or by downloading part models that were available from GrabCAD and orienting them using Mates in SolidWorks Assembly. I also created quick test prints of the retaining brackets and mounting holes to verify that my caliper measurements were accurate and that there was adequate interference so that components could be screwed directly into the 3D printed material. While assembling the pneumatic system, I performed bubble tests at every connection point to verify that no leaks had been introduced to the system. While soldering the electrical components, I used a digital multimeter to check that every component was receiving the expected supply voltage and that there were no shorts in the system. I then developed a custom GUI that allowed me to control each valve and the pump independently for the purpose of testing. This system allowed me to verify the functionality of the electrical system and to further verify the integrity of the pneumatic system. I could tell that the device worked as expected because I was able to pump up each quadrant of the cushion separately from one another and all of the quadrants held air which verified that there were no leaks.

Part A: Life-long Learning and Gaining of New Knowledge and Competence

Becoming a professional engineer requires a commitment to lifelong learning in order to contribute effectively and continue to uphold public welfare. During this past term I discovered that one such avenue for continuous growth involved learning about and applying emerging technologies such as additive manufacturing. In the past, I have worked with the Creality Ender-3 fused deposition modeling (FDM) 3D printer. This printer was very useful during the early prototyping stages of the project because it allowed us to test new part designs within a day. However, beyond the testing stage, both the manifold and custom spool component that I designed for this project required more precise manufacturing to avoid introducing leaks to the system. Since both of these parts have internal intersecting channels for airflow, they could not be manufactured using traditional metalworking techniques. As a workaround, the first option that I considered was to redesign the parts as multiple pieces that could be assembled after they had been individually manufactured out of metal. However, given the tight deadline of this project, this first option presented too much risk as there would not have been enough time for multiple design iterations if the addition of these new interfaces compromised the pneumatic integrity of the system. This led me to explore alternative additive manufacturing techniques where I learned about stereolithography (SLA) printers. During my reading, I learned that FDM printers bind the layers together mechanically whereas SLA printers create chemical bonds between layers which results in fully dense parts that are completely airtight [1]. The capabilities of SLA printers perfectly satisfied the needs of our project and thus I decided to pursue them further.

I learned that through the WATiMake MME Clinic, engineering students have access to Form 3+ SLA printers. In order to use those printers, I first completed the MAKE 100, 111, and 112 training modules which gave me an introduction to the WATiMake space and taught me the specifics about how SLA printers work and design/material selection techniques that would allow me to use this tool as effectively as possible. During these modules I also learned how to use the PreForm supporting software to setup the build plate and support my parts. I then attended a one-on-one in-person training session where I had the opportunity to walk through setting up a test print with a trainer. Once the print was complete, I learned how to post-process the part which included cleaning them with isopropyl alcohol and curing them in the cure bin. Throughout this training session I was cautioned about the many dangers associated with SLA resins and I made sure to follow all of the applicable safety protocols. Since the spool component proved to be a delicate part, I was able to practice my supporting and post-processing techniques using the Form 3+ printers each time we needed a new part. The time that I spent learning how to use these printers was instrumental to the success of our project as it allowed us to manufacture a final high-fidelity prototype that was void of leaks.

Part B: Teamwork

In my experience, an effective team is composed of teammates who possess the attributes of an ideal team player as outlined in Patrick Lencioni's book "The Ideal Team Player". These attributes include being *hungry*, *humble*, and *smart*. A *hungry* team player is someone who holds themselves to a high standard while completing their assigned individual tasks and also someone who actively seeks ways that they can contribute to bettering the team. According to Lencioni, a *humble* team player is not just someone who knows where they can improve upon their skills, but also someone who demonstrates the confidence in their abilities required to accomplish team goals. Lastly, a *smart* team player is an individual who has high emotional intelligence and who knows when it is time to engage in focused discussion. Throughout the duration of this project, our team has demonstrated the *hungry* and *humble* qualities of an ideal team player extremely well. Everyone has produced high quality work and has been eager to take on additional tasks to continue moving the project forward. We have also demonstrated humility by acknowledging our unique skills or gaps in our knowledge and by taking on related tasks or seeking guidance when appropriate. However, as a group we recognized early in the term that we were not exemplifying the *smart* quality as well as necessary leading us to implement impactful changes in our team's processes. During our team health assessment, we learned that as a team we needed to improve upon remaining focused during team meetings. We discussed different strategies and eventually decided to implement strict meeting agendas so that the objectives of our meetings were always clear. After executing this change within our collective Notion workspace, our meetings have become more efficient. Another byproduct of this change was that it provided a space for us to record and track our actionable items across multiple meetings.

As an individual I exemplify the *humility* trait well in that I know which skills I lack and which of my skills could benefit my team if used effectively. This was demonstrated by my choice to take on more electrical and mechanical design tasks rather than tasks related to algorithm design as I knew that my skills were better suited for that role. As a teammate, although I made significant contributions through many core design and development tasks throughout this project, I could perhaps have done a better job at being *hungry* for tasks that tend to garner less recognition and are not as appealing to me. An example of this is my reluctance to send outreach emails or fill out scholarship applications because I do not enjoy those writing tasks. Whereas I would have been a better team player if I contributed to those tasks especially because my teammates probably also did not enjoy them.

Part C: Professionalism and Practice

Professional biomedical engineers have a duty to prioritize public safety while engaging in the patient-centered design of novel medical devices. Professional engineers also have a duty to their employer to produce high-quality products that are cost-effective to manufacture. To accomplish this, they are expected to stay up to date on technological advancements and use their professional judgment during the concept selection phase of the engineering design process. As biomedical engineering students, we are also responsible for practicing the responsibilities of professional engineers during our design projects which give us an opportunity to learn from our mistakes before they can have more serious impacts on the public. Our design team's duty of care is owed not only to the end-users of our device (adult wheelchair users with complete spinal cord injuries who use air-filled cushions) but also to occupational therapists, caregivers, and family members of primary users. Due to the severe nature of pressure ulcers, any incompetence, negligence, misconduct, or unethical behavior during the design process by our team has the potential to be life-limiting or even life-threatening to an end-user. To mitigate such risks, during the development of our air-filled wheelchair cushion accessory device, our focus extended beyond innovation and encompassed adherence to ethical principles, regulatory requirements, and industry standards.

Since our project would be classified as a Class 2 medical device, we would have to demonstrate compliance with ISO 14971 for risk management and ISO 13485 for quality systems prior to receiving approval from Health Canada or any related regulatory bodies [2, 3]. Additionally, since our project is an electrical and pneumatic accessory to an existing wheelchair cushion, we would also have to demonstrate compliance with additional relevant medical device standards such as ISO 60601-1 for electrical safety, ISO 16840-2 for cushion comfort, support, and safety, and ISO 7176-19 for the selection, installation, and inspection of wheelchair seating systems, including cushions and accessories [4, 5, 6]. ISO 60601-1 was considered while designing the device housing to be water-resistant to splashes and incontinence, ISO 16840-2 was carefully considered while minimizing the size of the design of the spool component to avoid introducing new pressure points to the cushion system, and finally, ISO 7176-19 was considered while designing the wheelchair attachment mechanism to ensure security and robustness. In summary, our consideration of standards and careful design choices to prioritize user safety and satisfaction reflects our commitment to fulfilling the responsibilities of professional biomedical engineers while enhancing the quality of life of air-filled wheelchair cushion users.

References

- [1] A. Kafle, E. Luis, R. Silwal, H. M. Pan, P. L. Shrestha, and A. K. Bastola, “3D/4D Printing of polymers: Fused deposition modelling (FDM), selective laser sintering (SLS), and stereolithography (SLA),” *Polymers*, vol. 13, no. 18, p. 3101, 2021.
- [2] International Organization for Standardization, Medical devices – Application of risk management to medical devices, ISO 14971:2019(en) ed. Vernier, Geneva, Switzerland: International Organization for Standardization, 2019. [Online]. Available: <https://www.iso.org/standard/72704.html>
- [3] ——, Medical devices – Quality management systems – Requirements for regulatory purposes, ISO 13485:2016(en) ed. Vernier, Geneva, Switzerland: International Organization for Standardization, 2016. [Online]. Available: <https://www.iso.org/standard/59752.html>
- [4] ——, Wheelchair seating – Part 2: Determination of physical and mechanical characteristics of seat cushions intended to manage tissue integrity, ISO 16840-2:2018(en) ed. Vernier, Geneva, Switzerland: International Organization for Standardization, 2018. [Online]. Available: <https://www.iso.org/standard/66972.html>
- [5] ——, Medical electrical equipment – Part 1-11: General requirements for basic safety and essential performance – Collateral standard: Requirements for medical electrical equipment and medical electrical systems used in the home healthcare environment, IEC 60601-1-11:2015(en) ed. Vernier, Geneva, Switzerland: International Organization for Standardization, 2015. [Online]. Available: <https://www.iso.org/standard/65529.html>
- [6] ——, Wheelchairs – Part 19: Wheelchairs for use as seats in motor vehicles, ISO 7176-19:2022(en) ed. Vernier, Geneva, Switzerland: International Organization for Standardization, 2022. [Online]. Available: <https://www.iso.org/standard/71919.html>